IEEE Access
Multidisciplinary | Rapid Review | Open Access Journal

Received 17 November 2023, accepted 11 December 2023, date of publication 18 December 2023,
date of current version 27 December 2023.

Digital Object Identifier 10.1109/ACCESS.2023.3344561

RESEARCH ARTICLE

A New Family of Nyquist Pulses With Improved Performance

KYRIAKOS D. GAZOULEAS[1,2], NIKOS C. SAGIAS[2], (Senior Member, IEEE), MICHAEL C. BATISTATOS[2], AND KOSTAS P. PEPPAS[2], (Senior Member, IEEE)
[1]Department of Mathematics, National and Kapodistrian University of Athens (UoA), 157 84 Zografou, Greece
[2]Department of Informatics and Communications, University of Peloponnese, 221 00 Tripoli, Greece

Corresponding author: Kostas P. Peppas (peppas@uop.gr)

The publication of the article in OA mode was financially supported by HEAL-Link.

ABSTRACT In this work, we introduce and evaluate the performance of a novel family of Nyquist (intersymbol interference free) pulses that outperform several existing ones available in the open technical literature. The proposed pulse design is based on a polynomial interpolation approach, which - to the best of our knowledge - is applied for the first time for a Nyquist pulse. In particular, we propose a geometrical approach in conjunction with the use of cubic spline functions for the construction of the transfer function of the considered pulses. The proposed methodology is quite flexible, as it allows for the efficient design of Nyquist pulses with improved performance, even after the choice of the roll-off factor. Four members of the proposed family of pulses are studied in detail in terms of their frequency and time domain response, the eye diagram and the achieved bit error rate. The proposed theoretical analysis is corroborated by extensive numerically evaluated results. Our results have shown that for given values of the roll-off factor, the timing jitter and the signal to noise ratio, certain members of the proposed family can achieve a lower bit error rate as compared to several state-of-the-art pulses.

INDEX TERMS Intersymbol interference (ISI), Nyquist pulses, pulse shaping design, timing jitter.

I. INTRODUCTION

Next generation communication systems are expected to provide new types of enhanced user connectivity services, increased capacity, higher reliability, very high data rates, reduced latency, increased quality of service and availability as well as sophisticated applications, including high-fidelity holograms, immersive reality and industrial Internet of Things (IoT) [1], [2]. In order to support such applications, novel physical layer techniques achieving better bandwidth reuse and higher error-free data rates should be utilized.

Inter-symbol interference (ISI) is a major factor that degrades the error rate performance of a digital communication system. As shown in the pioneering work of Nyquist [3], a method to mitigate the deleterious impact of ISI on system performance is the design of appropriate pulses that guarantee transmission with minimum number of errors. Furthermore, the sensitivity of such pulse shaping filters to timing errors should be as low as possible [4]. The most popular design satisfying the above mentioned requirements is the so-called raised-cosine (RC) pulse [3], which has been widely employed in numerous practical digital communications systems, e.g. see [5], [6], [7], [8], [9], [10], and [11] and references therein.

For example, in [5], a linearly pulse modulation scheme has been proposed improve the performance of visible light communication (VLC) system. In [6], the impact of the roll-off factor, the side band suppression ratio and the ripple of sinc-shaped reconfigurable optical Nyquist pulse sequences has been investigated. In [7], the impact of the optical filter roll-off factor on Nyquist pulses generated by an on-chip silicon Mach-Zehnder modulator, has been investigated. In [8], a practical scheme to achieve reconfigurable optical frequency comb (OFC) and Nyquist pulses generation has been proposed. In [9], authors modeled a dual-parallel silicon modulator for sinc-shaped Nyquist pulse generation.

The associate editor coordinating the review of this manuscript and approving it for publication was Li Zhang.

In [10] authors proposed a sinc-Lorentzian Nyquist pulse shape for THz communications systems and experimentally demonstrated its performance. In [11], authors proposed and experimentally demonstrated a Nyquist pulse that can improve the error rate of a 311 GHz photonic-THz communications system.

On the other hand, the performance of digital receivers is also affected by the presence of timing jitter. Timing jitter results in deviations of the sampling points at the matched filter output from their optimal positions, thus further degrading error rate performance. In order to mitigate the undesired effects of jitter, the pulse tails should decay as quicky as possible outside the pulse interval.

The above mentioned considerations have motivated research on the development of improved ISI-free pulses that guarantee transmission with minimal number of errors while efficiently addressing the impact of jitter on error rate performance. Representative past examples can be found in [12], [13], [14], [15], [16], [17], [18], [19], [20], [21], [22], and [23].

Specifically, in [12], the so-called better than raised-cosine (BTRC) pulse has been proposed, which yields a larger eye opening and smaller symbol error rate than the conventional RC pulse. In [13], a parametric approach to construct families of ISI-free pulses in the frequency domain, has been presented. The pulses proposed in [12] and [13] have an explicit time-domain formula. Other improved pulses, that do not have an explicit time-domain expression are available in [14]. In that work, a family of ISI-free pulse-shaping filters with or without matched filtering have been proposed. In [15], two modified Nyquist pulses, namely the so-called flipped hyperbolic secant (fsech) and the flipped-inverse hyperbolic secant (farcsech) pulses. In the same work it has been shown that the farcsech pulse is systematically superior than the BTRC pulse, since it outperforms it in terms of symbol error rate and maximum distortion, in conjunction with an enhanced eye opening.

In [16], three alternative Nyquist pulses were devised that exploit the inherent flexibility of the concepts of inner and outer functions. Specifically, the proposed design was based on the use of the inverse cosine and the inverse hyperbolic sine function, as outer and inner function, respectively. In [17], improved parametric families of ISI-free pulses using the same concept, have been proposed. In that work, the proposed pulse design was based on the composition of the functions inverse cosine (outer function) and natural logarithm (inner function). In [18], an ISI-free pulse based on inverse-hyperbolic functions has been presented, which outperforms the ones proposed in [16] and [17].

A different pulse design approach has been adopted in [19], [20], [21], [22], [23], [24], [25], and [26]. In these works, additional design parameters have been included, whose values has been obtained using optimization techniques. Specifically, in [19] and [20], pulses with piece-wise parabolic and linear characteristics, respectively, have been proposed. In [24], two improved Nyquist filters with piece-wise rectangular-polynomial frequency characteristics have been presented and their performance has been analyzed. In [21], a pulse obtained from the linear combination of the RC and the BTRC pulses has been proposed. In [22], a family of ISI-free and band-limited polynomial pulses has been proposed. In [23], an ISI-free pulse has been proposed, whose roll-off characteristic is tunable with one power parameter. In [25], improved Nyquist pulses with transfer function that approximates a staircase frequency characteristic using spline functions have been proposed. In [26], an ISI-free pulse with piece-wise exponential frequency characteristic has been presented.

The performance of digital communication systems employing improved Nyquist pulses has further been addressed in several past research works, including [27], [28], [29], [30], [31], [32], [33], [34], [35], [36], [37] Further insights on the performance of several state-of-the-art pulses are available in [27]. In [28], a method of improving the error probability performance of various Nyquist pulses, by multiplying them with a specific compactly supported function, has been proposed. In [29], the concept of the so-called complementary Nyquist pulse has been proposed. In [30], a method to boost the performance of a Nyquist pulse in the presence of a timing error have been proposed. In [31], an approach using auxiliary factor has been proposed to remove ISI of Nyquist filters. In [32], a frequency domain design methodology for square-root Nyquist filters with low group delay and high and fast decaying stopband attenuation has been presented. In [33], the impact of improved Nyquist pulse shaping filters on the symbol error rate performance of generalized frequency division modulation (GFDM) systems has been addressed. The same authors, in [34], analyzed the impact of improved Nyquist pulse shaping filters on the physical layer performance of GFDM systems with Long Term Evolution-Advance (LTE-A) compatible frame structure. In [35], a real-time implementation of improved Nyquist pulse shape filters in carrier-less amplitude and phase (CAP) modulation in the context of a visible light communications system has been presented. In [36], the impact of carrier frequency offset on low latency-enabled unmanned aerial vehicles (UAV) using BTRC pulse shaping and GFDM, has been investigated. Finally, in [37], a comparison of most of the ISI-free pulses available in the open technical literature is performed, using a Pearson distance criterion.

Motivated by the above cited works, in this paper, we derive a new family of ISI-free pulses whose Fourier transform is obtained by employing a third degree polynomial approximation. Contrary to the two-parametric pulse designs, the proposed pulses invoke additional parameters obtained using a geometric approach. These parameters can be fine-tuned to improve the resulting error performance by using trial-and-error techniques. Despite the use of more than two-parameters, however, the resulting expressions for the transfer function of the proposed pulses are relatively

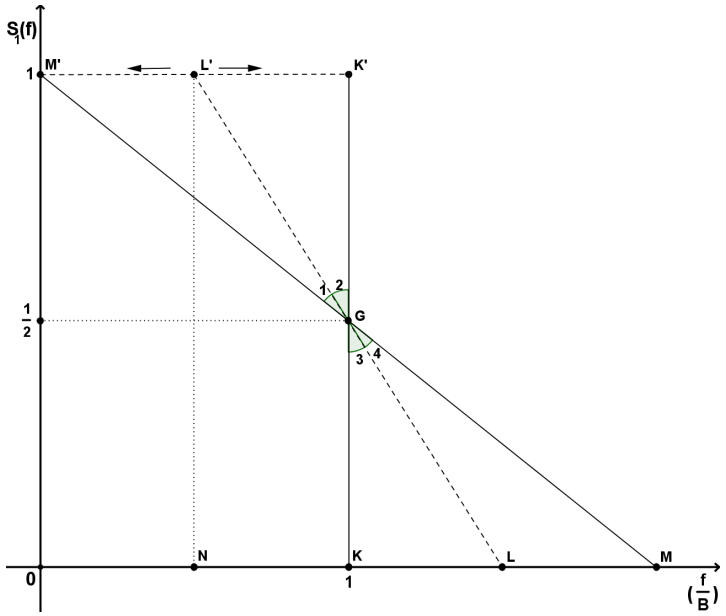

FIGURE 1. Geometric approach for the design of the first pulse: Basic concept.

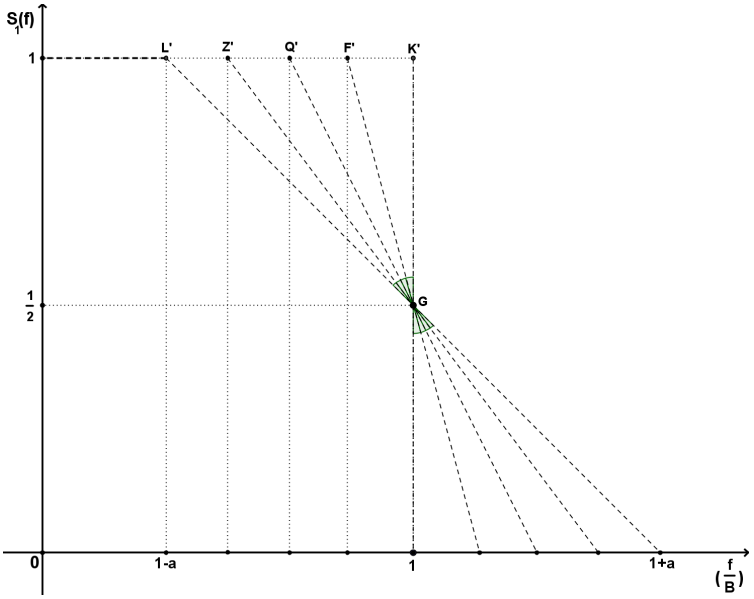

FIGURE 2. Complete geometric design of the first pulse.

simple, thus allowing for their efficient implementation in practical digital communication receivers. The performance of the proposed pulses is further analyzed in terms of their eye diagram and the achieved bit error rate. In particular, the contributions of this work are summarized as follows.

- We propose the use of a geometric approach in conjunction with a polynomial approximation using cubic spline functions to express the Fourier transform of the proposed family of pulses. The proposed design approach is motivated by the fact that cubic spline functions are smooth and do not exhibit the oscillatory behavior that characterizes high degree polynomial interpolation [38];
- We study in detail four representative members of the proposed family of pulses in terms of their frequency and time domain response and the eye diagram. The Fourier transform of the first pulse of interest can be expressed as a piece-wise linear function of the frequency, whereas for the remaining pulses the cubic spline approximation has been used;
- For given values of the roll-off factor, the time jitter and the signal-to-noise ratio, we analyze the performance of

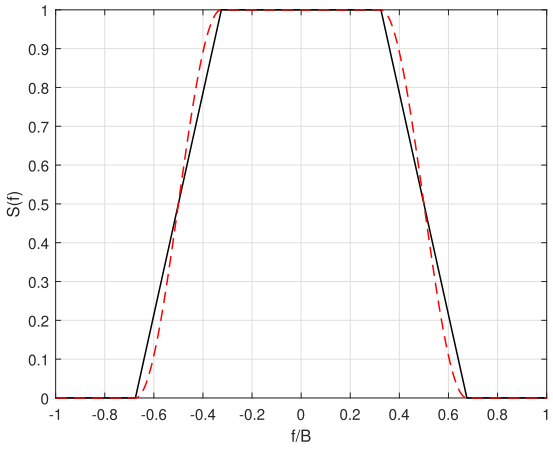

FIGURE 3. Transfer function of the first proposed pulse (continuous black line) and the RC pulse (dashed red line) for roll-off factor of 0.35.

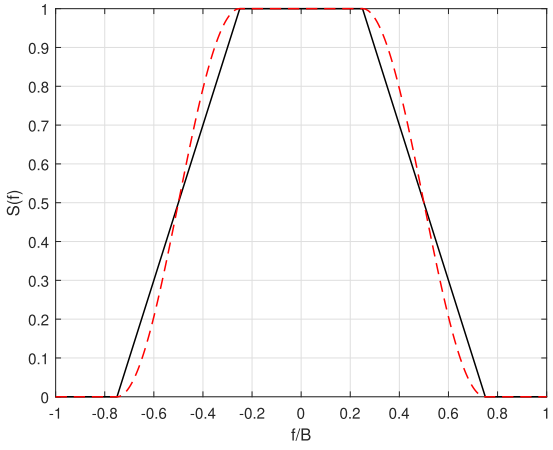

FIGURE 4. Transfer function of the first proposed pulse (continuous black line) and the RC pulse (dashed red line) for roll-off factor of 0.5.

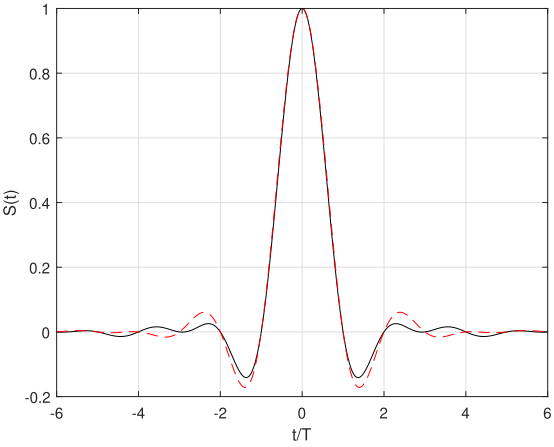

FIGURE 5. Impulse response of the first proposed pulse (continuous black line) and the RC pulse (dashed red line) for roll-off factor of 0.35.

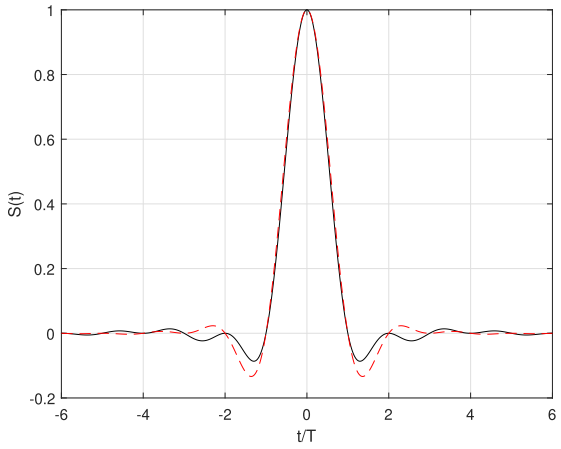

FIGURE 6. Impulse response of the first proposed pulse (continuous black line) and the RC pulse (dashed red line) for roll-off factor of 0.5.

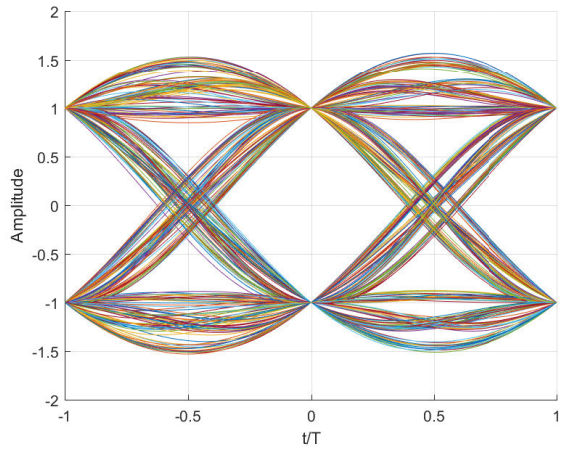

FIGURE 7. Eye diagram of the first proposed pulse for roll-off factor of 0.35.

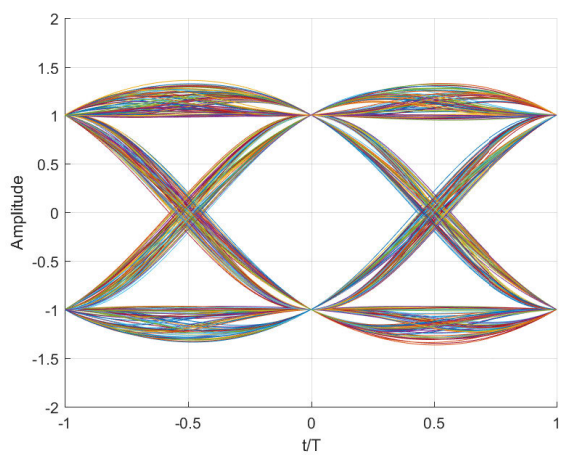

FIGURE 8. Eye diagram of the first proposed pulse for roll-off factor of 0.5.

the proposed pulses in terms of the achieved bit error rate and we compare it to the performance of state-of-the-art pulses;

Our numerical results have shown that the fourth member of the proposed family of pulses outperforms several of the best so far pulses available in the open technical literature, such as those proposed in [18].

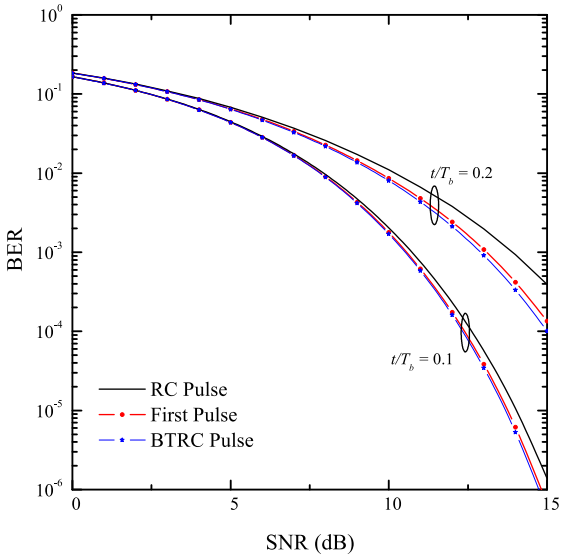

FIGURE 9. BER as a function of SNR in the presence of timing errors for RC, BTRC and the first proposed pulse for roll-off factor of 0.35.

II. MAIN RESULTS

In this section, we present in detail the geometrical construction of the four proposed pulses and analyze their performance in terms of the achieved bit error rate (BER).

A. GEOMETRICAL CONSTRUCTION OF THE FIRST PULSE

Fig 1 depicts the proposed geometric approach for the design of the first pulse. In this figure, it is assumed that point G is fixed. Let us construct the line segment LL' which passes through G. Obviously, points L and L' are variable. As it can be observed from Fig 1, point L' can move towards either M' or K' and thus, point L can move towards either M or K, respectively. It can be easily verified that the equation of the line MM' is $y = 1 - x/2$.

Let also $\beta \in [0, 1]$. It can be verified that the coordinates of M are $M(1 + \max\{\beta\}, 0)$. Similarly, the coordinates of M' are $M'(1 - \max\{\beta\}, 1)$. Furthermore, the coordinates of G are $G(1 + \max\{\beta\}, 1/2)$. Let now $L(x_1, 0)$ be the coordinates of L. Following a similar line of arguments, it can be deduced that $x_1 = 1 + a$, where $0 \leq a \leq \max\{\beta\}$, where a is the roll-off factor. By observing that triangles LKG and LKG' are congruent, it can further be deduced that $KL = K'L' = a$ and $M'L' = 1-a$. Thus, the coordinates of N and L are $N(1-a, 0)$ and $L(1+a, 0)$, respectively. In Fig. 2 the complete geometric design of the first pulse is depicted.

By inspecting Fig. 2, the transfer function of the first proposed pulse can be expressed as

$$S_1(f) = \begin{cases} T_b, & 0 \leq |f| \leq (1-a)B \\ -\dfrac{T_b}{2a}\left(\dfrac{|f|}{B} - 1 + a\right) + T_b, & (1-a)B \leq |f| \leq (1+a)B \\ 0, & |f| \geq (1+a)B \end{cases} \quad (1)$$

where B is the Nyquist frequency and $T_b = 1/(2B)$ is the bit interval.

Taking the inverse Fourier transform of (1) and after performing some algebraic manipulations, the impulse response of the first pulse can be expressed as in (2), shown at the bottom of the next page.

Figs. 3 and 4 depict the transfer function of the first proposed pulse (continuous black line) and the RC pulse (dashed red line) for roll-off factor of 0.35 and 0.5, respectively. The corresponding impulse responses are depicted in Figs. 5 and 6, respectively. It can be observed that –as expected– the impulse response of the proposed pulse is zero for integer multiples of t/T_b, thus satisfying the Nyquist criterion.

The achieved BER of the proposed pulse in the presence of timing errors can be computed analytically as [39]

$$P_b = \frac{1}{2} - \frac{2}{\pi} \sum_{\substack{m=1 \\ m:\ \text{odd}}}^{M} \frac{1}{m} \exp\left(-\frac{1}{2} m\omega^2\right) \sin(m\omega g_0) \times \prod_{\substack{k=N_1 \\ k\neq 0}}^{N_2} \cos(m\omega g_k). \quad (3)$$

In (3), M is the number of coefficients, $\omega = 2\pi/T_f$ where T_f is the period used in the series, N_1 and N_2 is the number of interfering symbols before and after the transmitted symbol, respectively, and $g_k = s(kT_b + \epsilon)$ where $s(t)$ is the pulse shape. Moreover, the signal-to-noise ratio can be expressed in terms of g_0 as $\text{SNR} = g_0^2$.

Fig. 9 depicts the achieved BER of the proposed first pulse, the RC and the BTRC pulses as a function of the SNR, for $a = 0.35$ and t/T_b of 0.1 and 0.2. As it can be observed, the proposed pulse outperforms the RC pulse whereas it performs slightly worse than the BTRC pulse for high SNR values. This motivates the extension of the proposed approach to design pulses with improved performance.

B. USING CUBIC POLYNOMIAL FUNCTIONS FOR THE GEOMETRICAL CONSTRUCTION OF PULSES WITH IMPROVED PERFORMANCE

The ideas behind the construction of pulses are based on the ideas presented in Figs. 1 and 2. However, in the geometric construction of the three new pulses, $S_j(f)$, $j = \{2, 3, 4\}$, instead of using a linear function that passes through points L', G and L, we propose the use of a piece-wise cubic polynomial function, $s_j(x)$, that pass through newly introduced points with coordinates (x_{ij}, y_{ij}), $2 \leq i \leq n$, where n is the number of the points.[1] The polynomial functions $s_j(x)$ can be expressed as (4), shown at the bottom page 9, where A_{ij}, B_{ij}, C_{ij} and D_{ij} are constant real parameters.

[1] As it will become evident later on, the proposed design approach is different to the approach proposed in [25]. Specifically, in [25], the so-called staircase characteristic has been adopted, using rectangles of equal width. The height of the rectangles has been determined by employing trial and error techniques that minimize the resulting error probability. In this work, the frequency characteristic design is based on a geometrical approach along with the use of cubic splines.

Since $s_j(x)$ and its first derivatives are continuous at $x = x_{ij}$, the parameters A_{ij}, B_{ij}, C_{ij} and D_{ij} can be evaluated as [38]

$$A_{ij} = \frac{y''_{i+1j} - y''_{ij}}{6h_{ij}} \tag{5a}$$

$$B_{ij} = \frac{y''_{ij}}{2} \tag{5b}$$

$$C_{ij} = \frac{y''_{i+1j} - y''_{ij}}{h_{ij}} - \frac{y''_{i+1j}\, h_{ij}}{6} - \frac{y''_{ij}\, h_{ij}}{3} \tag{5c}$$

$$D_{ij} = y_{ij} \tag{5d}$$

where $y_{ij} = s_j(x_{ij})$ and $h_{ij} = x_{i+1,j} - x_{ij}$. Moreover, the second derivatives y''_i can be obtained as the solution of the following linear system of equations

$$\mathbf{b} = \mathbf{E}\mathbf{y} \tag{6}$$

where $\mathbf{y} = [y''_{1j},\, y''_{2j}, \ldots y''_{nj}]^\dagger$ is the vector of the unknown derivatives y''_i and $\mathbf{E}$ is a tridiagonal matrix, whose main diagonal elements are given by the vector

$$\mathbf{d}_m = [u_1,\ 2\,(h_{1j} + h_{2j}),\ 2\,(h_{2j} + h_{3j}),\ \ldots,\ 2\,(h_{n-2,j} + h_{n-1,j}),\ u_n]^\dagger,$$

the elements of subdiagonal/lower diagonal are given by the vector

$$\mathbf{d}_l = [h_{1j},\, h_{2j}\, h_{3j}, \ldots, h_{n-2,j},\ 0]^\dagger,$$

and the elements of subdiagonal/upper diagonal by the vector

$$\mathbf{d}_u = [0,\ h_{2j},\ h_{3j}, \ldots, h_{n-2,j},\ h_{n-1,j}]^\dagger.$$

Finally, $\mathbf{b} = 6\,[u_3, b_{3j}, \ldots, b_{n,j}, u_4]^\dagger$ where

$$b_{ij} = \frac{y_{ij} - y_{i-1,j}}{h_{i-1,j}} - \frac{y_{i-1,j} - y_{i-2,j}}{h_{i-2,j}},\ 2 \le i \le n. \tag{7}$$

The coefficients u_1, u_2, u_3 and u_4 can be obtained using the initial conditions $y''_{1j} = 0$ and $y''_{nj} = 0$ as $u_1 = u_2 = 1$ and $u_3 = u_4 = 0$.

In the following sections, this concept will be applied to the design of pulses with improved performance.

C. GEOMETRIC DESIGN OF THE SECOND PULSE

The concept behind the design of the second pulse ($j = 2$) is depicted in Fig. 10. The main difference between the proposed design and the one shown in Figs. 1 and 2 is the addition of points with coordinates (x_2, y_2) and (x_4, y_4), where x_2, x_4 are fixed and y_2 and y_4 can freely move on y-axis to optimize error performance. Note that in Fig. 10 we have omitted the dependence of the coordinates from index j for brevity.

Hereafter, we select $x_2 = 1 - a/2$ and $x_4 = 1 + a/2$. It can be observed that the proposed geometrical construction exhibits odd symmetry about point (x_3, y_3), This is evident by observing that the coordinates of points (x_2, y_2) and (x_4, y_4) are $(1 - a/2, c_1)$ and $(1 + a/2, 1 - c_1)$, where $c_1 \in (1/2, 1)$. The above definition of the coordinates guarantees that the area of the proposed geometrical construction is a constant and independent to the value of the parameter c_1. It is further assumed that c_1 can be expressed using two decimal digits in order to simplify numerical computations, namely $c_1 = 0.51,\ 0.52, \ldots, 0.99$. Furthermore, it is assumed that the transfer function of the second proposed pulse satisfies the conditions $S_2((1-a)B) = 1$ and $S(B) = 1/2$.

Using the methodology described in the previous subsection, the proposed pulse will be designed by employing piece-wise cubic polynomials that pass through points (x_i, y_i), $i \in \{1, 2, 3, 4, 5\}$, with coordinates $(x_1, y_1) = (1 - a, 1)$, $(x_2, y_2) = (1 - a/2, c_1)$, $(x_3, y_3) = (1, 1/2)$, $(x_4, y_4) = (1+a/2, 1-c_1)$, $(x_5, y_5) = (1+a, 0)$. Specifically, the matrix $\mathbf{E}$ in (6) can be expressed as

$$\mathbf{E} = \begin{bmatrix} 1 & 0 & 0 & 0 & 0 \\ h_1 & 2(h_1+h_2) & h_2 & 0 & 0 \\ 0 & h_2 & 2(h_2+h_3) & h_3 & 0 \\ 0 & 0 & h_3 & 2(h_3+h_4) & h_4 \\ 0 & 0 & 0 & 0 & 1 \end{bmatrix} = \begin{bmatrix} 1 & 0 & 0 & 0 & 0 \\ a/2 & 2a & a/2 & 0 & 0 \\ 0 & a/2 & 2a & a/2 & 0 \\ 0 & 0 & a/2 & 2a & a/2 \\ 0 & 0 & 0 & 0 & 1 \end{bmatrix}. \tag{9}$$

Moreover, after performing some straightforward algebraic manipulations, vector $\mathbf{b}$ in (6) can be obtained as

$$\mathbf{b} = (24/a^2) \begin{bmatrix} 0 \\ y_3 - 2y_2 + y_1 \\ y_4 - 2y_3 + y_2 \\ y_5 - 2y_4 + y_3 \\ 0 \end{bmatrix} = (24/a^2) \begin{bmatrix} 0 \\ 3/2 - 2c_1 \\ 0 \\ 2c_1 - 3/2 \\ 0 \end{bmatrix} \tag{10}$$

$$\begin{aligned} s_1(t) = {} & \frac{T}{\pi\, t} \sin[2\,\pi\, t\, B\,(1-a)] + \frac{T}{4\,a\,B\,\pi^2\, t^2} \{\cos[2\,\pi\, t\, B\,(1-a)] - \cos[2\,\pi\, t\, B\,(1+a)]\} \\ & - \frac{T}{2\,a\,\pi\, t} \{(1+a)\, \sin[2\,\pi\, t\, B\,(1+a)] + (a-1)\, \sin[2\,\pi\, t\, B\,(1-a)]\} \\ & + \frac{T\,(a+1)}{2\,a\,\pi\, t} \{\sin[2\,\pi\, t\, B\,(1+a)] - \sin[2\,\pi\, t\, B\,(1-a)]\} \end{aligned} \tag{2}$$

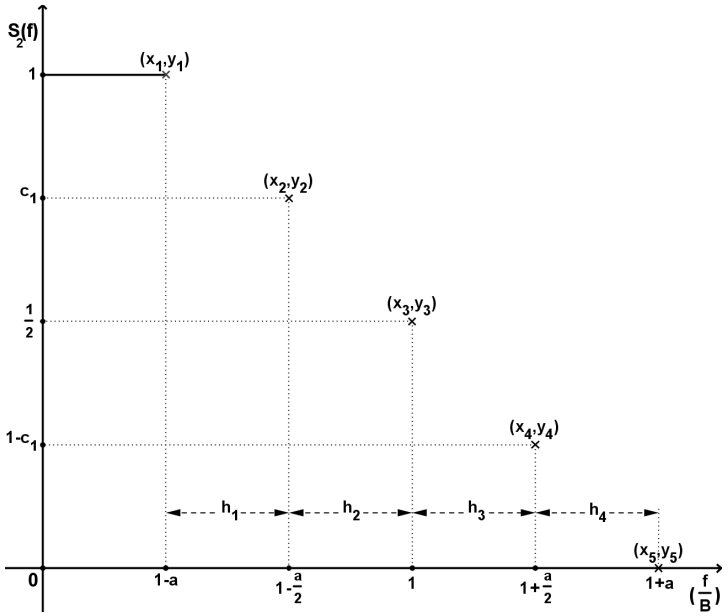

FIGURE 10. Geometric design of the second pulse.

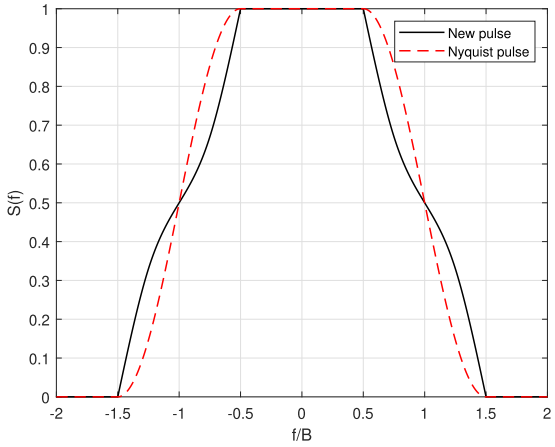

FIGURE 11. Transfer function of the second proposed pulse (continuous black line) and the RC pulse (dashed red line) for roll-off factor of 0.5 and c_1 of 0.67.

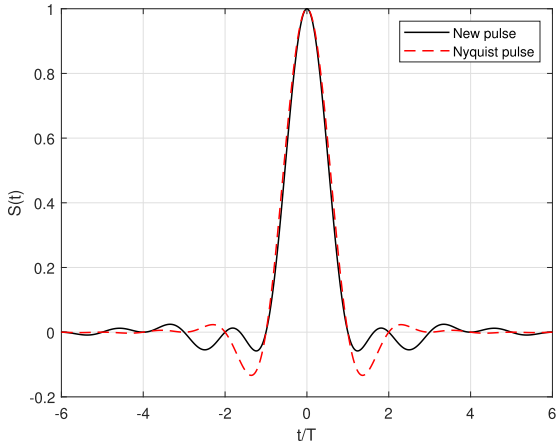

FIGURE 12. Impulse response of the second proposed pulse (continuous black line) and the RC pulse (dashed red line) for roll-off factor of 0.5 and c_1 of 0.67.

The solution of (6) is

$$\mathbf{y} = \begin{bmatrix} y_1'' \\ y_2'' \\ y_3'' \\ y_4'' \\ y_5'' \end{bmatrix} = \begin{bmatrix} 0 \\ (9-12c_1)/a^2 \\ 0 \\ (12c_1-9)/a^2 \\ 0 \end{bmatrix} \tag{11}$$

Let A_{i2}, B_{i2}, C_{i2}, D_{i2} be the coefficients of the cubic polynomial in (4). Using (5), these parameters can be readily obtained, yielding

$$\begin{bmatrix} A_{12} \\ B_{12} \\ C_{12} \\ D_{12} \end{bmatrix} = \begin{bmatrix} (3-4\,c_1)/a^3 \\ 0 \\ (12\,c_1-11)/(4\,a) \\ 1 \end{bmatrix} \tag{12a}$$

$$\begin{bmatrix} A_{22} \\ B_{22} \\ C_{22} \\ D_{22} \end{bmatrix} = \begin{bmatrix} (4\,c_1-3)/a^3 \\ (9-12\,c_1)/(2\,a^2) \\ -1/(2a) \\ c_1 \end{bmatrix} \tag{12b}$$

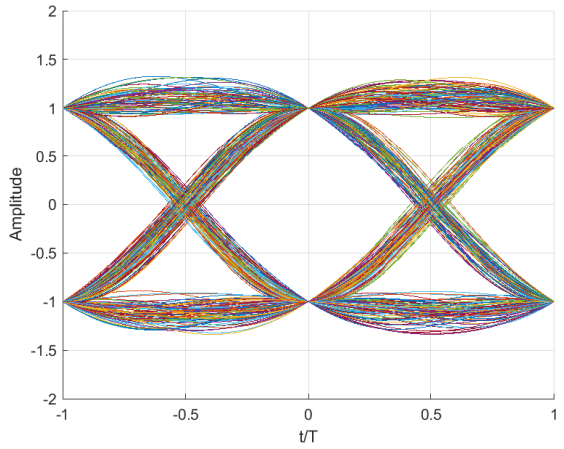

FIGURE 13. Eye Diagram of the second proposed pulse for roll-off factor of 0.5 and c_1 of 0.67.

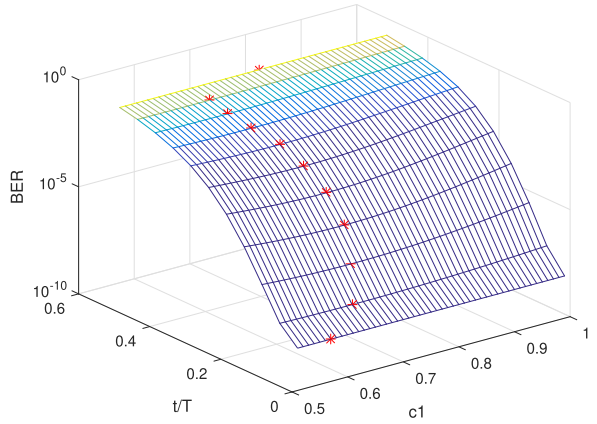

FIGURE 14. BER in the presence of timing errors for the second proposed pulse for SNR = 15 dB and $a = 0.25$, as a function of c_1 and the ratio t/T_b.

$$\begin{bmatrix} A_{32} \\ B_{32} \\ C_{32} \\ D_{32} \end{bmatrix} = \begin{bmatrix} (4c_1 - 3)/a^3 \\ 0 \\ (7 - 12c_1)/4a \\ 1/2 \end{bmatrix} \tag{12c}$$

$$\begin{bmatrix} A_{42} \\ B_{42} \\ C_{42} \\ D_{42} \end{bmatrix} = \begin{bmatrix} (3 - 4\,c_1)/a^3 \\ (12\,c_1 - 9)/(2\,a^2) \\ -1/(2\,a) \\ 1 - c_1 \end{bmatrix} \tag{12d}$$

The transfer function of the second pulse can finally be expressed as (8), shown at the bottom of the next page.

As it can be observed, the transfer function of the second pulse depends on the parameter c_1. This parameter can be suitably optimized so that the impact of jitter on the error probability is minimal.

Fig. 22 depicts the BER performance in the presence of timing errors for the second proposed pulse for SNR = 15 dB, 2^{10} interfering symbols and $a = 0.25$, as a function of c_1 and the timing jitter parameter, t/T_b. Clearly, for given values of t/T_b, BER attains a minimum value for a specific value of c_1. In Fig. 22, these values are depicted with red asterisks.

In Table 1, values of the BER for SNR = 15 dB and the corresponding values of c_1, are depicted, assuming different values of a and the ratio $\tau = |t/T_b|$. The values of c_1 have been obtained using a trial-and-error technique in order to obtain a close-to-minimum value of the error probability

Figs. 11 and 12 depict the transfer function and the impulse response of the proposed second pulse (continuous black line), respectively for roll-off factor of 0.5 and c_1 of 0.67. In the same diagrams similar results for the RC pulse (dashed red line) are also available. Clearly, the proposed pulse satisfies the Nyquist criterion, as its impulse response is zero for integer multiples of t/T_b. Moreover, as it can be observed, the side lobes of the impulse response of the proposed pulse are smaller that those of the RC pulse, thus revealing that the second pulse results in a better error performance that the RC pulse. For the same parameters a and c_1, Fig. 13 depicts the eye diagram of the second pulse. It is evident the eye is "open", and therefore the resulting bit error rate is small.

In the next section, the proposed geometrical construction will be extended to obtain pulses with even better performance.

D. GEOMETRIC DESIGN OF THE THIRD PULSE

Throughout the geometrical construction of the second pulse in Fig. 10, the x-coordinates of points (x_2, y_2) and (x_4, y_4) have been assumed fixed and the choice of their values arbitrary. In the proposed third pulse construction, we set $x_2 = k$ and $x_4 = 2 - k$, i.e. x_2 and x_4 are symmetric with respect to $x_3 = 1$. The corresponding geometrical construction is depicted in Fig. 15.

Let us define

$$k \triangleq 1 - a + \frac{1 - (1 - a)}{p_1} = 1 - a + \frac{a}{p_1}. \tag{15}$$

In (15), p_1 is a step parameter with $p_1 \in [2, 64]$, to facilitate implementation in a hardware based platform. Observe that for $p_1 = 1$, from (15) it holds that $k = 1$, i.e. point (x_2, y_2) is identical to (x_3, y_3), a situation not acceptable in Fig. 15. Moreover, for large values of p_1, i.e. $p_1 \to \infty$, it holds that $k = 1 - a$, i.e. i.e. point (x_2, y_2) is identical to (x_1, y_1). This situation is also not acceptable because of the finite precision of the hardware based platform. Thus, it always holds that $p_1 \leq 64$ for the proposed design. The coordinates of points (x_i, y_i) in Fig. 15 can be finally evaluated as $(x_1, y_1) = (1 - a.1)$, $(x_2, y_2) = (k, c_1)$, $(x_3, y_3) = (1, 1/2)$, $(x_4, y_4) = (2 - k, 1 - c_1)$, $(x_5, y_5) = (1 + a, 0)$. The matrix $\mathbf{E}$ and vector $\mathbf{b}$ in the system of equations (6) can thus be written as

$$\mathbf{E} = \begin{bmatrix} 1 & 0 & 0 & 0 & 0 \\ a+k-1 & 2a & 1-k & 0 & 0 \\ 0 & 1-k & 4-4k & 1-k & 0 \\ 0 & 0 & 1-k & 2a & a+k-1 \\ 0 & 0 & 0 & 0 & 1 \end{bmatrix} \tag{16}$$

and

$$\mathbf{b} = 6\begin{bmatrix} 0 \\ t_1 \\ 0 \\ -t_1 \\ 0 \end{bmatrix}, \tag{17}$$

respectively, where

$$t_1 = \frac{a - 2ac_1 - k + 1}{(2-2k)(a+k-1)}. \tag{18}$$

The solution of (6) is

$$\mathbf{y} = \begin{bmatrix} y_1'' \\ y_2'' \\ y_3'' \\ y_4'' \\ y_5'' \end{bmatrix} = \begin{bmatrix} 0 \\ 3t_1/a \\ 0 \\ -3t_1/a \\ 0 \end{bmatrix} \tag{19}$$

Let A_{i3}, B_{i3}, C_{i3}, D_{i3} be the coefficients of the cubic polynomial in (4). Using (5), these parameters can be readily obtained, yielding

$$\begin{bmatrix} A_{13} \\ B_{13} \\ C_{13} \\ D_{13} \end{bmatrix} = \begin{bmatrix} \frac{t_1}{2a(a+k-1)} \\ 0 \\ \frac{c_1-1}{a+k-1} + \frac{t_1(a+k-1)}{2a} \\ 1 \end{bmatrix} \tag{20a}$$

$$\begin{bmatrix} A_{23} \\ B_{23} \\ C_{23} \\ D_{23} \end{bmatrix} = \begin{bmatrix} \frac{t_1}{2a(k-1)} \\ \frac{3t_1}{2a} \\ \frac{1-2c_1}{2-2k} + \frac{t_1(k-1)}{a} \\ c_1 \end{bmatrix} \tag{20b}$$

$$\begin{bmatrix} A_{33} \\ B_{33} \\ C_{33} \\ D_{33} \end{bmatrix} = \begin{bmatrix} \frac{t_1}{2a(k-1)} \\ 0 \\ \frac{1-2c_1}{2-2k} + \frac{t_1(1-k)}{2a} \\ 1/2 \end{bmatrix} \tag{20c}$$

$$\begin{bmatrix} A_{43} \\ B_{43} \\ C_{43} \\ D_{43} \end{bmatrix} = \begin{bmatrix} \frac{t_1}{2a(a+k-1)} \\ -\frac{3t_1}{2a} \\ \frac{c_1-1}{a+k-1} + \frac{t_1(a+k-1)}{a} \\ 1 - c_1 \end{bmatrix} \tag{20d}$$

The transfer function of the third pulse can finally be expressed as (13).

Figs. 16 and 17 depict the transfer function of the proposed third pulse (continuous black line) assuming roll off factors of 0.35 and 0.5, respectively. The corresponding transfer functions of the traditional RC pulse are also depicted in the same figures (dashed red line). For the same values of the roll off factor, the impulse response of the third pulse is depicted in Figs. 18 ($a = 0.35$) and 19 ($a = 0.5$). Again, the side lobes of the impulse response are smaller than the corresponding ones of the second pulse, thus revealing that the proposed third pulse indeed performs better than the second one.

$$s_j(x) = \begin{cases} T_b, & 0 \le \frac{|f|}{B} \le x_{1j} \\ A_{1j}T_b\left(\frac{|f|}{B} - x_{1j}\right)^3 + B_{1j}T_b\left(\frac{|f|}{B} - x_{1j}\right)^2 + C_{1j}T_b\left(\frac{|f|}{B} - x_{1j}\right) + D_{1j}T_b, & x_{1j} \le \frac{|f|}{B} \le x_{2j} \\ A_{2j}T_b\left(\frac{|f|}{B} - x_{2j}\right)^3 + B_{2j}T_b\left(\frac{|f|}{B} - x_{2j}\right)^2 + C_{2j}T_b\left(\frac{|f|}{B} - x_{2j}\right) + D_{2j}T_b, & x_{2j} \le \frac{|f|}{B} \le x_{3j} \\ \cdots & \\ A_{n-1,j}T_b\left(\frac{|f|}{B} - x_{n-1,j}\right)^3 + B_{n-1,j}T_b\left(\frac{|f|}{B} - x_{n-1,j}\right)^2 + C_{n-1,j}T_b\left(\frac{|f|}{B} - x_{n-1,j}\right) + D_{n-1,j}T_b, & x_{n-1,j} \le \frac{|f|}{B} \le x_{n,j} \\ 0, & \frac{|f|}{B} \ge x_{n,j} \end{cases} \tag{4}$$

$$S_2(f) = \begin{cases} T_b, \ 0 \le |f| \le (1-a)B \\ A_{12}\,T_b\left(\frac{|f|}{B} - 1 + a\right)^3 + C_{12}\,T_b\left(\frac{|f|}{B} - 1 + a\right) + D_{12}T_b, \ (1-a)B \le |f| \le (1-\frac{a}{2})B \\ A_{22}\,T_b\left(\frac{|f|}{B} - 1 + \frac{a}{2}\right)^3 + B_{22}\,T_b\left(\frac{|f|}{B} - 1 + \frac{a}{2}\right)^2 + C_{22}\,T_b\left(\frac{|f|}{B} - 1 + \frac{a}{2}\right) + D_{22}\,T_b, \ \left(1 - \frac{a}{2}\right)B \le |f| \le B \\ A_{32}\,T_b\left(\frac{|f|}{B} - 1\right)^3 + C_{32}\,T_b\left(\frac{|f|}{B} - 1\right) + D_{32}\,T_b, \ \ B \le |f| \le \left(1 + \frac{a}{2}\right)B \\ A_{42}\,T_b\left(\frac{|f|}{B} - 1 - \frac{a}{2}\right)^3 + B_{42}\,T_b\left(\frac{|f|}{B} - 1 - \frac{a}{2}\right)^2 + C_{42}\,T_b\left(\frac{|f|}{B} - 1 - \frac{a}{2}\right) + D_{42}\,T_b, \ \left(1 + \frac{a}{2}\right)B \le |f| \le (1+a)\,B \\ 0, \ \ |f| \ge (1+a)\,B \end{cases} \tag{8}$$

TABLE 1. BER in the presence of timing errors for the second proposed pulse for SNR = 15 dB and the corresponding values of c_1, for different values of a and the ratio $\tau = |t/T_b|$.

a	$\tau = 0.05$	$\tau = 0.1$	$\tau = 0.2$	$\tau = 0.25$	$\tau = 0.3$
0.2	$c_1 = 0.53$ 6.51×10^{-8}	$c_1 = 0.56$ 1.75×10^{-6}	$c_1 = 0.57$ 5.45×10^{-4}	$c_1 = 0.56$ 4.15×10^{-3}	$c_1 = 0.54$ 1.81×10^{-2}
0.25	$c_1 = 0.55$ 5.21×10^{-8}	$c_1 = 0.58$ 1.08×10^{-6}	$c_1 = 0.6$ 2.87×10^{-4}	$c_1 = 0.59$ 2.39×10^{-3}	$c_1 = 0.58$ 1.21×10^{-2}
0.35	$c_1 = 0.58$ 3.54×10^{-8}	$c_1 = 0.61$ 4.67×10^{-7}	$c_1 = 0.63$ 8.80×10^{-5}	$c_1 = 0.63$ 8.15×10^{-4}	$c_1 = 0.63$ 5.14×10^{-3}
0.5	$c_1 = 0.61$ 2.23×10^{-8}	$c_1 = 0.64$ 1.69×10^{-7}	$c_1 = 0.67$ 2.04×10^{-5}	$c_1 = 0.68$ 1.98×10^{-4}	$c_1 = 0.68$ 1.56×10^{-3}
0.75	$c_1 = 0.68$ 1.38×10^{-8}	$c_1 = 0.68$ 4.51×10^{-8}	$c_1 = 0.71$ 3.31×10^{-6}	$c_1 = 0.73$ 3.99×10^{-5}	$c_1 = 0.75$ 4.49×10^{-4}
1	$c_1 = 0.76$ 1.23×10^{-8}	$c_1 = 0.75$ 2.96×10^{-8}	$c_1 = 0.75$ 1.35×10^{-6}	$c_1 = 0.76$ 1.87×10^{-5}	$c_1 = 0.78$ 2.64×10^{-4}

Finally, the eye diagrams are depicted in Figs. 20 ($a = 0.35$) and 21 ($a = 0.5$). It can be observed that the eye opening is larger than the one of the second pulse, thus further verifying that the third pulse yields better error performance than the second one.

Fig. 22 depicts the achieved BER of the third pulse in the presence of timing errors, assuming SNR of 15 dB, roll-off factor of 0.5, 2^{10} interfering symbols, t/T_b of 0.2, as a function of parameters c_1 and p_1. As it is evident, BER attains a minimum value, depicted with an asterisk. Table 2 depicts the achieved BER of the third proposed pulse and the corresponding values of c_1 and p_1 for which BER attains its specific value, for various values of $\tau \triangleq |t/T_b|$ and a. Again, c_1 and p_1 have been deduced by employing trial-and-error techniques to in order to get a close-to-optimal value of the error probability. In what follows an even better pulse will be designed and its performance will be analyzed in detail.

$$S_3(f) = \begin{cases} T_b, \ 0 \le |f| \le (1-a)B \\ A_{13}T_b\left(\frac{|f|}{B} - 1 + a\right)^3 + C_{13}T_b\left(\frac{|f|}{B} - 1 + a\right) + D_{13}T_b, \ (1-a)B \le |f| \le kB \\ A_{23}T_b\left(\frac{|f|}{B} - k\right)^3 + B_{23}T_b\left(\frac{|f|}{B} - k\right)^2 + C_{23}T_b\left(\frac{|f|}{B} - k\right) + D_{23}T_b, \ kB \le |f| \le B \\ A_{33}T_b\left(\frac{|f|}{B} - 1\right)^3 + C_{33}T_b\left(\frac{|f|}{B} - 1\right) + D_{33}T_b, \quad B \le |f| \le (2-k)B \\ A_{43}T_b\left(\frac{|f|}{B} - 2 + k\right)^3 + B_{43}T_b\left(\frac{|f|}{B} - 2 + k\right)^2 + C_{43}T_b\left(\frac{|f|}{B} - 2 + k\right) + D_{43}T_b, \ (2-k)\,B \le |f| \le (1+a)B \\ 0, \quad |f| \ge (1+a)B \end{cases} \tag{13}$$

$$S_4(f) = \begin{cases} T_b, \ 0 \le |f| \le (1-a)B \\ A_{14}T_b\left(\frac{|f|}{B} - 1 + a\right)^3 + B_{14}T_b\left(\frac{|f|}{B} - 1 + a\right)^2 + C_{14}T_b\left(\frac{|f|}{B} - 1 + a\right) + D_{14}T_b, \ (1-a)B \le |f| \le kB \\ A_{24}T_b\left(\frac{|f|}{B} - k\right)^3 + B_{24}T_b\left(\frac{|f|}{B} - k\right)^2 + C_{24}T_b\left(\frac{|f|}{B} - k\right) + D_{24}T_b, \ kB \le |f| \le dB \\ A_{34}T_b\left(\frac{|f|}{B} - d\right)^3 + B_{34}T_b\left(\frac{|f|}{B} - d\right)^2 + C_{34}T_b\left(\frac{|f|}{B} - d\right) + D_{34}T_b, \quad dB \le |f| \le B \\ A_{44}T_b\left(\frac{|f|}{B} - 1\right)^3 + B_{44}T_b\left(\frac{|f|}{B} - 1\right)^2 + C_{44}T_b\left(\frac{|f|}{B} - 1\right) + D_{44}T_b, \ B \le |f| \le (2-d)B \\ A_{54}T_b\left(\frac{|f|}{B} - 2 + d\right)^3 + B_{54}T_b\left(\frac{|f|}{B} - 2 + d\right)^2 + C_{54}T_b\left(\frac{|f|}{B} - 2 + d\right) + D_{54}T_b. \ (2-d)B \le |f| \le (2-k)B \\ A_{64}T_b\left(\frac{|f|}{B} - 2 + k\right)^3 + B_{64}T_b\left(\frac{|f|}{B} - 2 + k\right)^2 + C_{64}T_b\left(\frac{|f|}{B} - 2 + k\right) + D_{64}T_b. \ (2-k)B \le |f| \le (1+a)B \\ 0, \quad |f| \ge (1+a)B \end{cases} \tag{14}$$

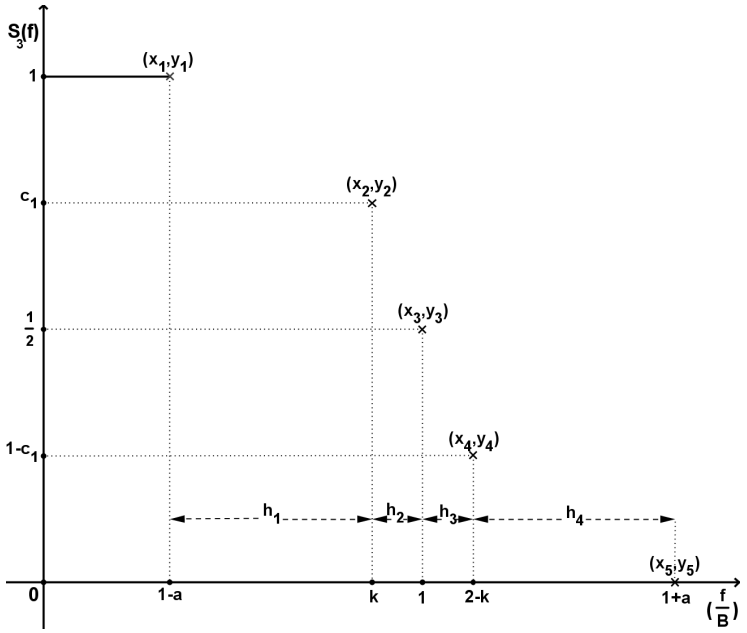

FIGURE 15. Geometric design of the third pulse.

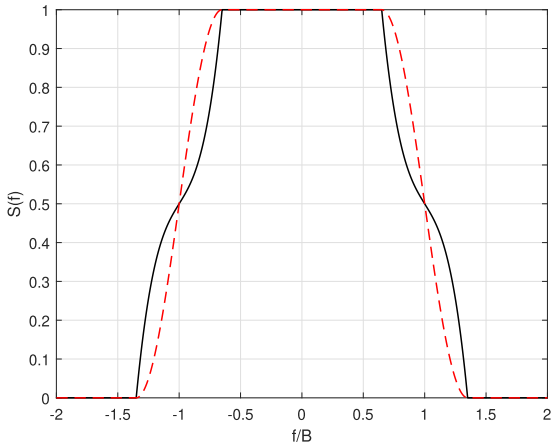

FIGURE 16. Transfer function of the third proposed pulse (continuous black line) and the RC pulse (dashed red line) for roll-off factor of 0.35, p_1 of 56 and c_1 of 0.98.

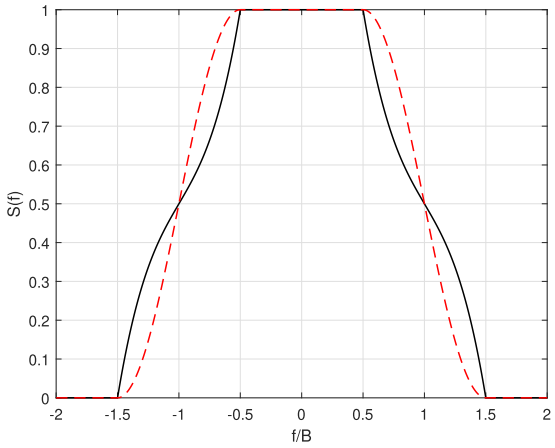

FIGURE 17. Transfer function of the third proposed pulse (continuous black line) and the RC pulse (dashed red line) for roll-off factor of 0.5, p_1 of 47 and c_1 of 0.98.

E. GEOMETRIC DESIGN OF THE FOURTH PULSE

Hereafter, we further elaborate on the proposed geometrical construction to design a fourth pulse yielding an even better performance than the previously proposed ones. The concept behind the geometrical design of the proposed fourth pulse is depicted in Fig. 23.

As shown in Fig. 23, we define $(x_3, y_3) = (d, c_2)$ with $1/2 < c_2 < c_1$ and $(x_5, y_5) = (2 - d, 1 - c_2)$. Parameter d is defined as $d = k + (1 - k)/p_2$ where P_2 is positive integer. Observe that if $p_2 = 1$ then $d_1 = 1$ and therefore, points (x_3, y_3), (x_5, y_5) and (x_4, y_4) would be identical, a contradiction. Again, it holds that $S_4(B) = 1/2$ and $S_4((1-a)B) = 1$. Moreover, the area of the graph of the transfer function is again a constant and equal to one.

Based on Fig. 23, the coordinates of points (x_i, y_i), $i \in \{1, 2, \ldots, 7\}$, can be obtained as $(x_1, y_1) = (1 - a, 1)$, $(x_2y_2) = (k, c_1)$, $(x_3, y_3) = (d, c_2)$, $(x_4, y_4) = (1, 1/2)$, $(x_5, y_5) = (2 - d, 1 - c_2)$, $(x_6, y_6) = (2 - k, 1 - c_1)$ and $(x_7, y_7) = (1 + a, 0)$. Let us define the parameters.

$$r_1 = \frac{kc_2 + ac_2 - ac_1 - c_2 + c_1 - dc_1 + d - k}{(d - k)(a + k - 1)} \tag{21}$$

and

$$r_2 = \frac{d - k + 2kc_2 + 2c_1 - 2c_2 - 2dc_1}{(2 - 2d)(d - k)}. \tag{22}$$

After performing some tedious, yet straightforward algebraic manipulations, the coefficients of the piece-wise cubic

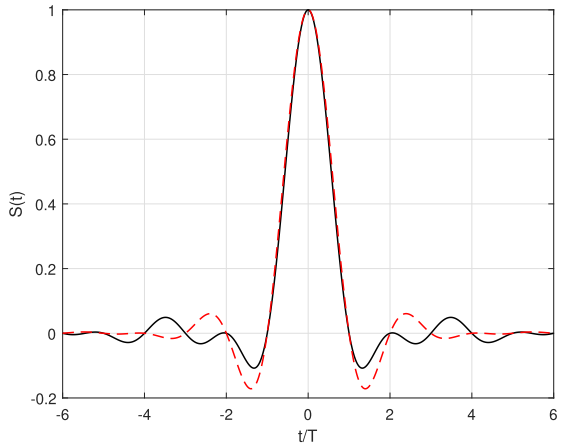

FIGURE 18. Impulse response of the third proposed pulse (continuous black line) and the RC pulse (dashed red line) for roll-off factor of 0.35, p_1 of 56 and c_1 of 0.98.

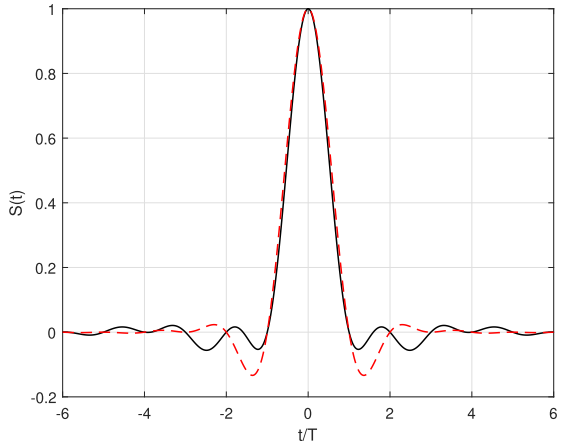

FIGURE 19. Impulse response of the third proposed pulse (continuous black line) and the RC pulse (dashed red line) for roll-off factor of 0.5, p_1 of 47 and c_1 of 0.98.

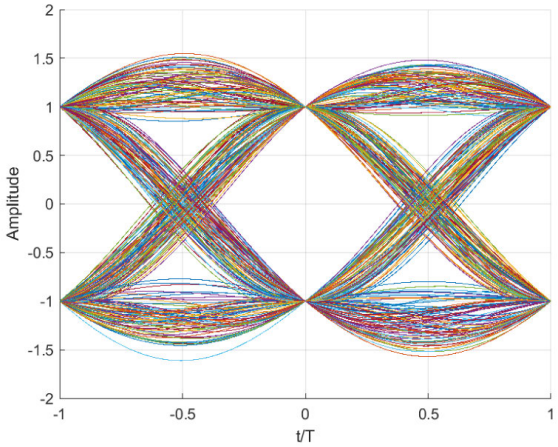

FIGURE 20. Eye Diagram of the third proposed pulse for roll-off factor of 0.35, p_1 of 56 and c_1 of 0.98.

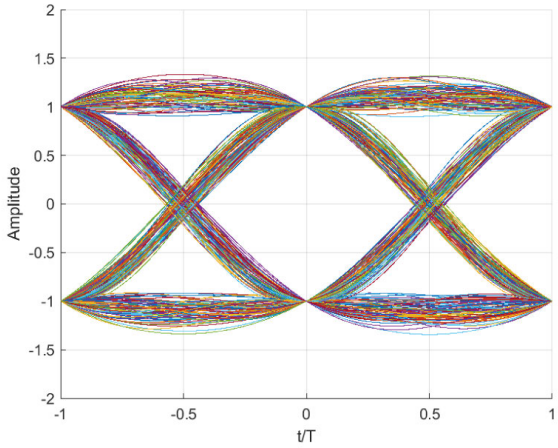

FIGURE 21. Eye Diagram of the third proposed pulse for roll-off factor of 0.5, p_1 of 47 and c_1 of 0.98.

polynomial given by the solution of the system in (6) can be deduced as

$$\begin{bmatrix} A_{14} \\ B_{14} \\ C_{14} \\ D_{14} \end{bmatrix} = \begin{bmatrix} \frac{-2r_1+2kr_1+dr_2-kr_2}{(4-4a-4d+d^2-4k+4ak+2dk+k^2)(a+k-1)} \\ 0 \\ \frac{(-2r_1+2kr_1+dr_2-kr_2)(a+k-1)}{4-4a-4d+d^2-4k+4ak+2dk+k^2} + \frac{c_1-1}{a+k-1} \\ 1 \end{bmatrix} \tag{23a}$$

$$\begin{bmatrix} A_{24} \\ B_{24} \\ C_{24} \\ D_{24} \end{bmatrix} = \begin{bmatrix} \frac{dr_1-3kr_1+2r_2-2ar_2-3dr_2+2r_1+kr_2}{(4-4a-4d+d^2-4k+4ak+2dk+k^2)(d-k)} \\ \frac{3(-2r_1+2kr_1+dr_2-kr_2)}{4-4a-4d+d^2-4k+4ak+2dk+k^2} \\ \frac{c_2-c_1}{d-k} + \frac{(-dr_1-3kr_1-2r_2+2ar_2+4r_1+2kr_2)(d-k)}{4-4a-4d+d^2-4k+4ak+2dk+k^2} \\ c_1 \end{bmatrix} \tag{23b}$$

$$\begin{bmatrix} A_{34} \\ B_{34} \\ C_{34} \\ D_{34} \end{bmatrix} = \begin{bmatrix} \frac{(-dr_1+kr_1-2r_2+2ar_2+2dr_2)}{(4-4a-4d+d^2-4k+4ak+2dk+k^2)(1-d)} \\ \frac{-3(-dr_1+kr_1-2r_2+2ar_2+2dr_2)}{4-4a-4d+d^2-4k+4ak+2dk+k^2} \\ \frac{1-2c_2}{2-2d} + \frac{2(-dr_1+kr_1-2r_2+2ar_2+2dr_2)(1-d)}{4-4a-4d+d^2-4k+4ak+2dk+k^2} \\ c_2 \end{bmatrix} \tag{23c}$$

$$\begin{bmatrix} A_{44} \\ B_{44} \\ C_{44} \\ D_{44} \end{bmatrix} = \begin{bmatrix} \frac{-dr_1+kr_1-2r_2+2ar_2+2dr_2}{(4-4a-4d+d^2-4k+4ak+2dk+k^2)(1-d)} \\ 0 \\ \frac{1-2c_2}{2-2d} + \frac{(dr_1-kr_1+2r_2-2ar_2-2dr_2)(1-d)}{4-4a-4d+d^2-4k+4ak+2dk+k^2} \\ 1/2 \end{bmatrix} \tag{23d}$$

$$\begin{bmatrix} A_{54} \\ B_{54} \\ C_{54} \\ D_{54} \end{bmatrix} = \begin{bmatrix} \frac{dr_1-3kr_1+2r_2-2ar_2-3dr_2+2r_1+kr_2}{(4-4a-4d+d^2-4k+4ak+2dk+k^2)(d-k)} \\ \frac{-3(dr_1-kr_1+2r_2-2ar_2-2dr_2)}{4-4a-4d+d^2-4k+4ak+2dk+k^2} \\ \frac{c_2-c_1}{d-k} + \frac{(-2r_1-3dr_2-kr_2+2dr_1+4r_2-4ar_2)(d-k)}{4-4a-4d+d^2-4k+4ak+2dk+k^2} \\ 1-c_2 \end{bmatrix} \tag{23e}$$

$$\begin{bmatrix} A_{64} \\ B_{64} \\ C_{64} \\ D_{64} \end{bmatrix} = \begin{bmatrix} \frac{-2r_1+2kr_1+dr_2-kr_2}{(4-4a-4d+d^2-4k+4ak+2dk+k^2)(a+k-1)} \\ \frac{-3(-2r_1+2kr_1+dr_2-kr_2)}{4-4a-4d+d^2-4k+4ak+2dk+k^2} \\ \frac{c_1-1}{a+k-1} + \frac{2(-2r_1+2kr_1+dr_2-kr_2)(a+k-1)}{4-4a-4d+d^2-4k+4ak+2dk+k^2} \\ 1-c_1 \end{bmatrix} \tag{23f}$$

The transfer function of the fourth proposed pulse can finally be expressed as (14).

TABLE 2. BER in the presence of timing errors for the third proposed pulse for SNR = 15 dB, 2^{10} interfering symbols and the corresponding values of c_1 and p_1, for different values of a and the ratio $\tau = |t/T_b|$.

a	$\tau = 0.05$	$\tau = 0.1$	$\tau = 0.2$	$\tau = 0.25$	$\tau = 0.3$
0.2	$c_1 = 0.97$ $p_1 = 55$ 6.31×10^{-8}	$c_1 = 0.97$ $p_1 = 50$ 1.64×10^{-6}	$c_1 = 0.97$ $p_1 = 48$ 5.03×10^{-4}	$c_1 = 0.97$ $p_1 = 50$ 3.87×10^{-3}	$c_1 = 0.97$ $p_1 = 53$ 1.72×10^{-2}
0.25	$c_1 = 0.97$ $p_1 = 52$ 5.03×10^{-8}	$c_1 = 0.58$ $p_1 = 47$ 1.01×10^{-6}	$c_1 = 0.6$ $p_1 = 44$ 2.62×10^{-4}	$c_1 = 0.59$ $p_1 = 45$ 2.21×10^{-3}	$c_1 = 0.58$ $p_1 = 47$ 1.13×10^{-2}
0.35	$c_1 = 0.97$ $p_1 = 47$ 3.41×10^{-8}	$c_1 = 0.98$ $p_1 = 62$ 4.35×10^{-7}	$c_1 = 0.98$ $p_1 = 56$ 8.00×10^{-5}	$c_1 = 0.98$ $p_1 = 56$ 7.44×10^{-4}	$c_1 = 0.98$ $p_1 = 58$ 4.76×10^{-3}
0.5	$c_1 = 0.98$ $p_1 = 64$ 2.15×10^{-8}	$c_1 = 0.98$ $p_1 = 57$ 1.56×10^{-7}	$c_1 = 0.98$ $p_1 = 47$ 1.86×10^{-5}	$c_1 = 0.98$ $p_1 = 45$ 1.83×10^{-4}	$c_1 = 0.98$ $p_1 = 44$ 1.46×10^{-3}
0.75	$c_1 = 0.98$ $p_1 = 44$ 1.36×10^{-8}	$c_1 = 0.98$ $p_1 = 44$ 4.29×10^{-8}	$c_1 = 0.98$ $p_1 = 35$ 3.15×10^{-6}	$c_1 = 0.99$ $p_1 = 62$ 3.90×10^{-5}	$c_1 = 0.99$ $p_1 = 54$ 4.46×10^{-4}
1	$c_1 = 0.98$ $p_1 = 23$ 1.23×10^{-8}	$c_1 = 0.97$ $p_1 = 16$ 2.95×10^{-8}	$c_1 = 0.99$ $p_1 = 51$ 1.35×10^{-6}	$c_1 = 0.76$ $p_1 = 2$ 1.87×10^{-5}	$c_1 = 0.78$ $p_1 = 2$ 2.64×10^{-4}

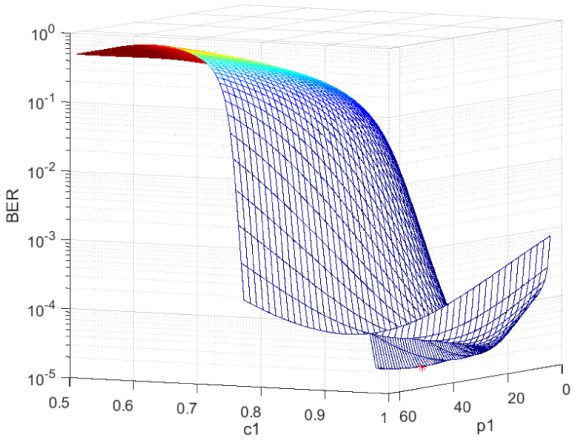

FIGURE 22. BER in the presence of timing errors for the third proposed pulse for SNR = 15 dB, 2^{10} interfering symbols, $t/T_b = \pm 0.2$ and $a = 0.5$, as a function of c_1 and p_1.

Figs. 24, 26 and 28 depict the transfer function, the impulse response and the eye diagram, respectively, of the proposed fourth pulse (continuous black line) assuming roll off factor of 0.35, p_1 of 60, c_1 of 0.85, c_2 of 0.79 and p_2 of 38. The corresponding transfer functions of the traditional RC pulse are also depicted in the same figures (dashed red line).

Moreover, Figs. 25 and 27 and 29 depict the transfer function, the impulse response and the eye diagramm, respectively, of the proposed fourth pulse (continuous black line) assuming roll off factor of 0.5, p_1 of 60, c_1 of 0.85, c_2 of 0.82 and p_2 of 64. The corresponding transfer functions of the traditional RC pulse are also depicted in the same figures (dashed red line).

By the observation of Figs. 26 and 27, it becomes evident that, once again, the side lobes of the impulse response of the fourth pulse are again smaller than the corresponding ones of the third pulse, thus, verifying the performance enhancements provided by the proposed fourth design. Similar findings can be verified by the observation of the eye diagrams in Figs. 28 and 29, i.e. the eye opening is larger than the one of the third pulse.

Table 3 presents BER performance results for the fourth pulse in the presence of timing errors, assuming fixed values of c_1 and p_1 and variable c_2 and p_2, for SNR of 15 dB, 2^{10} interfering symbols and various values of τ. For the specific test case it is assumed that $p_1 = 60$ and $c_1 = 0.85$. Again, the values of c_2 and p_2 have been obtained using a trial-and-error approach. This pulse achieves an improved BER performance as compared to the previously proposed ones with reasonable implementation complexity.

In an effort to further improve the performance of the fourth pulse at the cost of implementation complexity, variable values of c_i and p_i are assumed, $\forall i \in \{1, 2\}$. The resulting BER values and the corresponding values of of c_i and p_i are available in Table 4. As it is obvious, the fourth pulse outperforms the proposed third pulse in terms of the achieved BER, even in the case of fixed c_1 and p_1. In what follows we compare the error performance of the proposed pulses with the one provided by several state-of-the-art pulses, available in the open technical literature.

Table 5 depicts the error performance of the proposed third and fourth pulses and compares their performance with state-of-the-art two-parametric pulses proposed in [16], [17], and [18], for SNR of 15 dB, roll-off factor of 0.2 and various values of τ. Note that the motivation behind the selection of a small value of a is that such a value is preferable for forthcoming communication systems, because of the fact that a small value of a results in lower bandwidth. As it can be observed, the third pulse yields a better error performance than the pulses acos[log] and acos[sinh] proposed in [16] and [17], however, its performance is worse than the best so far two-parameter pulse available in the open technical literature, acsch[asech], proposed in [18]. Nevertheless, the proposed fourth pulse $s_4(t)$, with $p_1 = 60$ and $c_1 = 0.85$ outperforms the acsch[asech] pulse for all considered values of τ. The superior performance of the proposed pulse stems from the

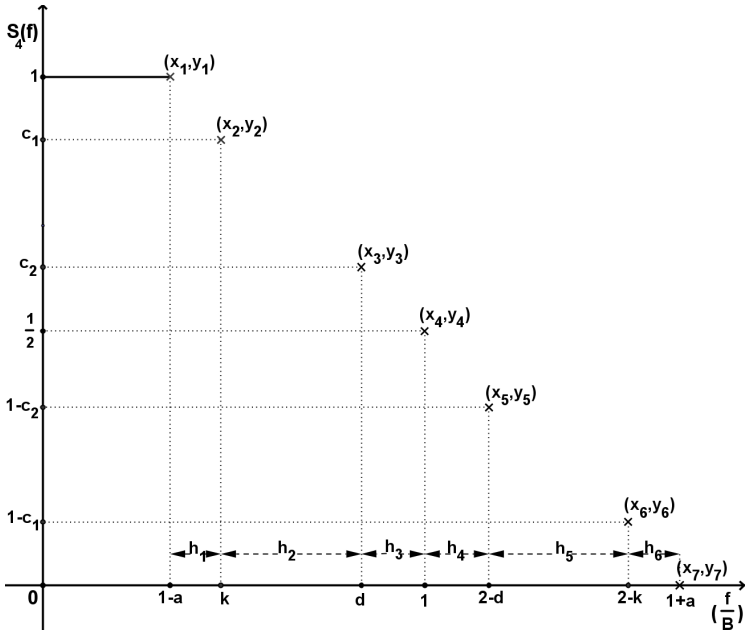

FIGURE 23. Geometric design of the fourth pulse.

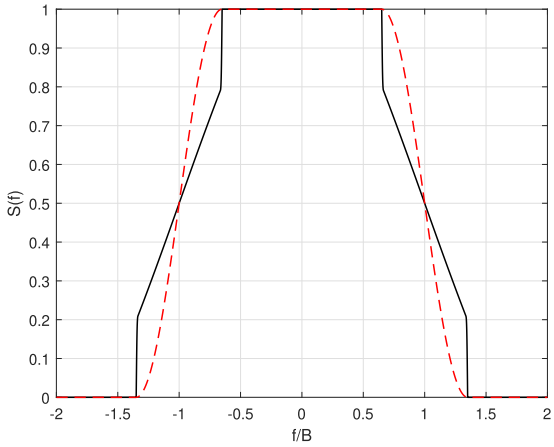

FIGURE 24. Transfer function of the fourth proposed pulse (continuous black line) and the RC pulse (dashed red line) for roll-off factor of 0.35, p_1 of 60, c_1 of 0.85, c_2 of 0.79 and p_2 of 38.

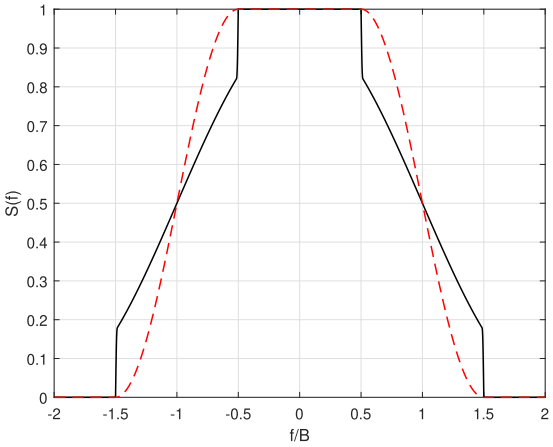

FIGURE 25. Transfer function of the fourth proposed pulse (continuous black line) and the RC pulse (dashed red line) for roll-off factor of 0.5, p_1 of 60, c_1 of 0.85, c_2 of 0.82 and p_2 of 64.

fact that the proposed geometrical approach using piece-wise cubic polynomials allows for better control of the dominant side lobes than the compared pulses, which in turn have adopted the approach of inner-outer functions. Even better BER results have been reported for the improved fourth pulse with variable values of c_1, p_1, c_2 and p_2.

In what follows, we compare the proposed ISI-free pulses with both two-parametric pulses as well as with pulses employing more than two parameters. Tables 6 and 7 compare the performance of several two-parametric ISI-free pulses available in the open technical literature, namely the RC, BTRC (also known as fexp [15]), fsech [15], farcsech [15], Poly [21], acos [17], acos[acos] [17], acos[asech] [17], acos[log] [17], asech[acos] [17], asech[asech] [17], asech[log] [17], asech [exp] [17], acos[exp] [17] acos[asinh] [16], acos[atan] [16], sin[acosh] [16], as well as of pulses employing more than two parameters, namely the Power [23] and the Poly [22], with the fourth and the improved fourth proposed pulse. In Table 6, it is assumed that $\alpha = 0.25$ whereas in Table 7, $\alpha = 0.35$. BER results for the pulses with which comparison is carried out are available in [27, Table 5] and [27, Table 6], for $\alpha = 0.25$ and $\alpha = 0.35$, respectively. Note that the Poly and Power pulses, as well as the proposed pulses do not not have a fixed form for a given value of α but depend on one, three, or four parameters, respectively. As it can be observed, both the standard as well as the improved fourth proposed pulse, outperform all the considered pulses in terms of BER performance.

Next, we compare the propose pulse designs with ones employing multiple parameters, namely those proposed in [25] and [22]. In Table 8, the BER performance of the standard and the improved fourth pulses is compared with that

TABLE 3. BER in the presence of timing errors for the fourth proposed pulse for SNR = 15 dB, 2^{10} interfering symbols, $p_1 = 60$, $c_1 = 0.85$ and the corresponding values of c_2 and p_2, for different values of a and the ratio $\tau = |t/T_b|$.

a	$\tau = 0.05$	$\tau = 0.1$	$\tau = 0.2$	$\tau = 0.25$	$\tau = 0.3$
0.2	$c_2 = 0.63$ $p_2 = 12$ 5.80×10^{-8}	$c_2 = 0.65$ $p_2 = 13$ 1.37×10^{-6}	$c_2 = 0.72$ $p_2 = 20$ 3.98×10^{-4}	$c_2 = 0.71$ $p_2 = 19$ 3.17×10^{-3}	$c_2 = 0.66$ $p_2 = 14$ 1.48×10^{-2}
0.25	$c_2 = 0.66$ $p_2 = 14$ 4.58×10^{-8}	$c_2 = 0.72$ $p_2 = 20$ 8.21×10^{-7}	$c_2 = 0.74$ $p_2 = 23$ 1.98×10^{-4}	$c_2 = 0.74$ $p_2 = 23$ 1.72×10^{-3}	$c_2 = 0.72$ $p_2 = 20$ 9.34×10^{-3}
0.35	$c_2 = 0.72$ $p_2 = 20$ 3.07×10^{-8}	$c_2 = 0.75$ $p_2 = 25$ 3.47×10^{-7}	$c_2 = 0.79$ $p_2 = 38$ 5.78×10^{-5}	$c_2 = 0.79$ $p_2 = 38$ 5.45×10^{-4}	$c_2 = 0.79$ $p_2 = 38$ 3.67×10^{-3}
0.5	$c_2 = 0.75$ $p_2 = 25$ 1.92×10^{-8}	$c_2 = 0.77$ $p_2 = 30$ 1.19×10^{-7}	$c_2 = 0.82$ $p_2 = 64$ 1.30×10^{-5}	$c_2 = 0.82$ $p_2 = 63$ 1.33×10^{-4}	$c_2 = 0.82$ $p_2 = 62$ 1.13×10^{-3}
0.75	$c_2 = 0.82$ $p_2 = 62$ 1.31×10^{-8}	$c_2 = 0.82$ $p_2 = 62$ 3.79×10^{-8}	$c_2 = 0.82$ $p_2 = 60$ 2.76×10^{-6}	$c_2 = 0.82$ $p_2 = 58$ 3.89×10^{-5}	$c_2 = 0.82$ $p_2 = 57$ 4.94×10^{-4}
1	$c_2 = 0.82$ $p_2 = 53$ 1.47×10^{-8}	$c_2 = 0.82$ $p_2 = 54$ 5.12×10^{-8}	$c_2 = 0.82$ $p_2 = 56$ 2.77×10^{-6}	$c_2 = 0.82$ $p_2 = 57$ 2.76×10^{-5}	$c_2 = 0.82$ $p_2 = 59$ 2.77×10^{-4}

TABLE 4. BER in the presence of timing errors for the improved fourth proposed pulse for SNR = 15 dB, 2^{10} interfering symbols, for different values of a and the ratio $\tau = |t/T_b|$.

α	$\tau = 0.05$	$\tau = 0.1$	$\tau = 0.2$	$\tau = 0.25$	$\tau = 0.3$
0.2	$p_1 = 62$ $c_1 = 0.69$ $p_2 = 63$ $c_2 = 0.63$ 5.75×10^{-8}	$p_1 = 72$ $c_1 = 0.75$ $p_2 = 64$ $c_2 = 0.69$ 1.35×10^{-6}	$p_1 = 69$ $c_1 = 0.75$ $p_2 = 61$ $c_2 = 0.69$ 3.90×10^{-4}	$p_1 = 79$ $c_1 = 0.75$ $p_2 = 62$ $c_2 = 0.68$ 3.11×10^{-3}	$p_1 = 67$ $c_1 = 0.72$ $p_2 = 64$ $c_2 = 0.66$ 1.47×10^{-2}
0.25	$p_1 = 56$ $c_1 = 0.71$ $p_2 = 62$ $c_2 = 0.66$ 4.55×10^{-8}	$p_1 = 65$ $c_1 = 0.76$ $p_2 = 64$ $c_2 = 0.71$ 8.10×10^{-7}	$p_1 = 64$ $c_1 = 0.78$ $p_2 = 60$ $c_2 = 0.73$ 1.96×10^{-4}	$p_1 = 66$ $c_1 = 0.77$ $p_2 = 63$ $c_2 = 0.72$ 1.70×10^{-3}	$p_1 = 64$ $c_1 = 0.76$ $p_2 = 63$ $c_2 = 0.7$ 9.22×10^{-3}
0.35	$p_1 = 63$ $c_1 = 0.75$ $p_2 = 64$ $c_2 = 0.7$ 3.04×10^{-8}	$p_1 = 65$ $c_1 = 0.8$ $p_2 = 57$ $c_2 = 0.75$ 3.43×10^{-7}	$p_1 = 60$ $c_1 = 0.82$ $p_2 = 58$ $c_2 = 0.78$ 5.74×10^{-5}	$p_1 = 67$ $c_1 = 0.82$ $p_2 = 64$ $c_2 = 0.78$ 5.42×10^{-4}	$p_1 = 60$ $c_1 = 0.82$ $p_2 = 58$ $c_2 = 0.78$ 3.65×10^{-3}
0.5	$p_1 = 60$ $c_1 = 0.79$ $p_2 = 64$ $c_2 = 0.75$ 1.91×10^{-8}	$p_1 = 64$ $c_1 = 0.81$ $p_2 = 64$ $c_2 = 0.77$ 1.18×10^{-7}	$p_1 = 60$ $c_1 = 0.85$ $p_2 = 64$ $c_2 = 0.82$ 1.30×10^{-5}	$p_1 = 66$ $c_1 = 0.87$ $p_2 = 64$ $c_2 = 0.84$ 1.32×10^{-4}	$p_1 = 63$ $c_1 = 0.87$ $p_2 = 61$ $c_2 = 0.84$ 1.12×10^{-3}
0.75	$p_1 = 60$ $c_1 = 0.9$ $p_2 = 51$ $c_2 = 0.87$ 1.30×10^{-8}	$p_1 = 68$ $c_1 = 0.9$ $p_2 = 57$ $c_2 = 0.87$ 3.67×10^{-8}	$p_1 = 70$ $c_1 = 0.91$ $p_2 = 53$ $c_2 = 0.88$ 2.43×10^{-6}	$p_1 = 76$ $c_1 = 0.93$ $p_2 = 48$ $c_2 = 0.9$ 3.17×10^{-5}	$p_1 = 75$ $c_1 = 0.93$ $p_2 = 64$ $c_2 = 0.91$ 3.87×10^{-4}
1	$p_1 = 50$ $c_1 = 0.99$ $p_2 = 46$ $c_2 = 0.98$ 1.23×10^{-8}	$p_1 = 50$ $c_1 = 0.99$ $p_2 = 47$ $c_2 = 0.98$ 2.95×10^{-8}	$p_1 = 95$ $c_1 = 0.99$ $p_2 = 5$ $c_2 = 0.88$ 1.30×10^{-6}	$p_1 = 89$ $c_1 = 0.95$ $p_2 = 61$ $c_2 = 0.93$ 1.65×10^{-5}	$p_1 = 99$ $c_1 = 0.93$ $p_2 = 59$ $c_2 = 0.9$ 2.21×10^{-4}

of the spline (Spline 3) and staircase pulses ($X_3(f)$ and $X_4(f)$), proposed in [25]. In the same table, results for the polynomial pulse (Poly), proposed in [22], are also presented. As it can be observed, the fourth pulse outperforms the spline pulse in terms of the achieved BER for all considered cases. As far as the comparison of the fourth pulse with the staircase pulse, $X_3(f)$, is concerned, it can be observed that for $\alpha = 0.25$, the fourth pulse performs slightly worse than $X_3(f)$ for all values of τ. Specifically, for $\tau = 0.05$, bit error probabilities of 4.58×10^{-8} and 4.55×10^{-8} have been reported for the standard and the improved fourth pulse, respectively. For the same test case, $X_3(f)$ achieves a BER of 4.52×10^{-8}. For the same α and τ of 0.1, the error probabilities obtained by the standard and improved fourth pulses are 8.21×10^{-7} and 8.10×10^{-7}, respectively, whereas $X_3(f)$ achieves a BER of 8.07×10^{-7}.

For $\alpha = 0.35$ and $\tau = 0.05$, the BER performance gap between the fourth pulse and $X_3(f)$ is even smaller. For the specific test scenario, bit error probabilities of 3.07×10^{-8} and 3.04×10^{-8} have been reported for the standard and the

TABLE 5. Comparative BER performance of the third pulse, $s_3(t)$, the fourth pulse, $s_4(t)$ ($p_1 = 60$, $c_1 = 0.85$) and the improved fourth pulse, with those proposed in [16], [17], and [18], for various values of $\tau \triangleq |t/T_b|$, SNR = 15dB and $a = 0.2$.

Pulse	$\tau = 0.05$	$\tau = 0.1$	$\tau = 0.2$	$\tau = 0.3$
acos[log] [16], [17]	6.72×10^{-8}	1.80×10^{-6}	5.55×10^{-4}	1.90×10^{-2}
acos[asinh] [16], [17]	6.51×10^{-8}	1.69×10^{-6}	5.10×10^{-4}	1.80×10^{-2}
acsch[asech] [18]	6.26×10^{-8}	1.54×10^{-6}	4.54×10^{-4}	1.68×10^{-2}
	6.31×10^{-8}	1.64×10^{-6}	5.03×10^{-4}	1.72×10^{-2}
$s_3(t)$	$c_1 = 0.97$	$c_1 = 0.97$	$c_1 = 0.97$	$c_1 = 0.97$
	$p_1 = 55$	$p_1 = 50$	$p_1 = 48$	$p_1 = 53$
	$\mathbf{5.80 \times 10^{-8}}$	$\mathbf{1.37 \times 10^{-6}}$	$\mathbf{3.98 \times 10^{-4}}$	$\mathbf{1.48 \times 10^{-2}}$
$s_4(t)$	$p_2 = 12$	$p_2 = 13$	$p_2 = 20$	$p_2 = 14$
	$c_2 = 0.63$	$c_2 = 0.65$	$c_2 = 0.72$	$c_2 = 0.66$
	$\mathbf{5.75 \times 10^{-8}}$	$\mathbf{1.35 \times 10^{-6}}$	$\mathbf{3.90 \times 10^{-4}}$	$\mathbf{1.47 \times 10^{-2}}$
	$p_1 = 62$	$p_1 = 72$	$p_1 = 69$	$p_1 = 67$
$s_4(t)$ (improved)	$c_1 = 0.69$	$c_1 = 0.75$	$c_1 = 0.75$	$c_1 = 0.72$
	$p_2 = 63$	$p_2 = 64$	$p_2 = 61$	$p_2 = 64$
	$c_2 = 0.63$	$c_2 = 0.69$	$c_2 = 0.69$	$c_2 = 0.66$

TABLE 6. Comparative BER performance of the fourth pulse, $s_4(t)$ ($p_1 = 60$, $c_1 = 0.85$) and the improved fourth pulse, with those available in [27, Table 5], for various values of $\tau \triangleq |t/T_b|$, SNR = 15dB and $\alpha = 0.25$.

Pulse (α= 0.25)	$\tau = 0.05$	$\tau = 0.1$	$\tau = 0.2$
rcos	8.22×10^{-8}	2.82×10^{-6}	9.75×10^{-4}
fsech	7.56×10^{-8}	2.33×10^{-6}	7.72×10^{-4}
asech[log]	6.17×10^{-8}	1.48×10^{-6}	4.26×10^{-4}
fexp	5.81×10^{-8}	1.30×10^{-6}	3.57×10^{-4}
farcsech	5.40×10^{-8}	1.10×10^{-6}	2.84×10^{-4}
acos[log]	5.33×10^{-8}	1.07×10^{-6}	2.74×10^{-4}
acos[atan]	5.31×10^{-8}	1.06×10^{-6}	2.71×10^{-4}
sin[acosh]	5.29×10^{-8}	1.06×10^{-6}	2.69×10^{-4}
acos[asinh]	5.15×10^{-8}	9.98×10^{-7}	2.49×10^{-4}
acos[exp]	5.10×10^{-8}	9.81×10^{-7}	2.44×10^{-4}
acos[asech]	5.07×10^{-8}	9.68×10^{-7}	2.40×10^{-4}
acos	5.06×10^{-8}	9.66×10^{-7}	2.39×10^{-4}
acos[acos]	4.95×10^{-8}	9.26×10^{-7}	2.27×10^{-4}
asech[exp]	4.92×10^{-8}	9.18×10^{-7}	2.25×10^{-4}
asech[asech]	4.87×10^{-8}	9.01×10^{-7}	2.21×10^{-4}
asech[acos]	4.87×10^{-8}	9.01×10^{-7}	2.21×10^{-4}
Poly (39, -99, 85)	4.76×10^{-8}	8.82×10^{-7}	2.21×10^{-4}
Power ($\beta = 0.29$)	4.62×10^{-8}	8.28×10^{-7}	2.03×10^{-4}
	$\mathbf{4.58 \times 10^{-8}}$	$\mathbf{8.21 \times 10^{-7}}$	$\mathbf{1.98 \times 10^{-4}}$
$s_4(t)$	$p_2 = 14$	$p_2 = 20$	$p_2 = 23$
	$c_2 = 0.66$	$c_2 = 0.72$	$c_2 = 0.74$
	$\mathbf{4.55 \times 10^{-8}}$	$\mathbf{8.10 \times 10^{-7}}$	$\mathbf{1.96 \times 10^{-4}}$
	$p_1 = 56$	$p_1 = 65$	$p_1 = 64$
$s_4(t)$ (improved)	$c_1 = 0.71$	$c_1 = 0.76$	$c_1 = 0.78$
	$p_2 = 62$	$p_2 = 64$	$p_2 = 60$
	$c_2 = 0.66$	$c_2 = 0.71$	$c_2 = 0.73$

improved fourth pulse, respectively. The corresponding BER achieved by $X_3(f)$ is 3.03×10^{-8}, i.e. $X_3(f)$ performs very close to the improved fourth pulse. For the same value of α and τ of 0.1, both the standard and the improved fourth pulses slightly outperform $X_3(f)$.

Finally, for $\alpha = 0.5$ and $\tau = 0.05$, the standard fourth pulse performs almost identically to $X_3(f)$ whereas the improved fourth pulse slightly outperforms $X_3(f)$. For $\tau = 0.05$, both the standard and the improved pulses yield a better error performance than $X_3(f)$.

Finally, comparisons of the proposed pulse designs with the multi-parameter pulses proposed in [19], [22], [26], and [23] will be presented. Comparisons with several two-parameter pulses, namely those available in [16] and [17] are also included. In Table 9, comparative BER performance of the fourth pulse, $s_4(t)$ ($p_1 = 60, c_1 = 0.85$) and the improved fourth pulse, with those available in [26, Table 6] are presented, for various values of $\tau \triangleq |t/T_b|$ and α with SNR = 15dB. The following pulses are considered: piecewise flipped exponential (PFE) [26], optimized PFE [26], poly [22], power [23], acos[asinh] [16], asech[asech] [17], and CC3 [19] pulses. Firstly, it is evident that both the standard as well the improved fourth pulse outperform the poly, the power, the acos[asinh], the asech[asech] and the CC3 pulses. As far as the PFE pulse is concerned, it can be observed that the standard PFE pulse performs slightly better than the standard fourth pulse for τ of 0.05 and all considered values of α. Nevertheless the performance gap between both considered pulses is very small. For larger values of τ, the standard fourth pulse performs better than the standard PFE pulse for all considered values of α. Moreover, as α increases, the performance gap between both considered pulses increase.

TABLE 7. Comparative BER performance of the fourth pulse, $s_4(t)$ ($p_1 = 60$, $c_1 = 0.85$) and the improved fourth pulse, with those available in [27, Table 6], for various values of $\tau \triangleq |t/T_b|$, SNR = 15dB and $\alpha = 0.35$.

Pulse (α= 0.35)	$\tau = 0.05$	$\tau = 0.1$	$\tau = 0.2$
rcos	6.00×10^{-8}	1.39×10^{-6}	3.91×10^{-4}
fsech	5.40×10^{-8}	1.09×10^{-6}	2.80×10^{-4}
asech[log]	4.21×10^{-8}	6.29×10^{-7}	1.26×10^{-4}
fexp	3.93×10^{-8}	5.40×10^{-7}	1.01×10^{-4}
farcsech	3.60×10^{-8}	4.46×10^{-7}	7.62×10^{-5}
acos[log]	3.55×10^{-8}	4.34×10^{-7}	7.35×10^{-5}
acos[atan]	3.53×10^{-8}	4.30×10^{-7}	7.28×10^{-5}
sin[acosh]	3.52×10^{-8}	4.27×10^{-7}	7.22×10^{-5}
acos[asinh]	3.41×10^{-8}	4.04×10^{-7}	6.77×10^{-5}
acos[exp]	3.38×10^{-8}	3.98×10^{-7}	6.66×10^{-5}
acos[asech]	3.36×10^{-8}	3.93×10^{-7}	6.56×10^{-5}
acos	3.35×10^{-8}	3.92×10^{-7}	6.58×10^{-5}
Poly (31, -80, 69)	3.29×10^{-8}	3.84×10^{-7}	6.56×10^{-5}
Poly (53, -134,113)	3.21×10^{-8}	4.13×10^{-7}	8.77×10^{-5}
Poly (36, -93,80	3.25×10^{-8}	3.79×10^{-7}	6.61×10^{-5}
Poly (30.59, -78.27, 67.2)	3.28×10^{-8}	3.82×10^{-7}	6.55×10^{-5}
acos[acos]	3.28×10^{-8}	3.80×10^{-7}	6.43×10^{-5}
asech[exp]	3.26×10^{-8}	3.78×10^{-7}	6.44×10^{-5}
asech[acos]	3.23×10^{-8}	3.74×10^{-7}	6.45×10^{-5}
asech[asech]	3.23×10^{-8}	3.73×10^{-7}	6.41×10^{-5}
Power ($\beta = 0.4$)	3.17×10^{-8}	3.63×10^{-7}	6.22×10^{-5}
Power ($\beta = 0.23$)	3.05×10^{-8}	3.70×10^{-7}	7.40×10^{-5}
Power ($\beta = 0.32$)	3.10×10^{-8}	3.55×10^{-7}	6.43×10^{-5}
Power ($\beta = 0.39$)	3.16×10^{-8}	3.61×10^{-7}	6.19×10^{-5}
	$\mathbf{3.07 \times 10^{-8}}$	$\mathbf{3.47 \times 10^{-7}}$	$\mathbf{5.78 \times 10^{-5}}$
$s_4(t)$	$p_2 = 20$	$p_2 = 25$	$p_2 = 38$
	$c_2 = 0.72$	$c_2 = 0.75$	$c_2 = 0.79$
	$\mathbf{3.04 \times 10^{-8}}$	$\mathbf{3.43 \times 10^{-7}}$	$\mathbf{5.74 \times 10^{-5}}$
	$p_1 = 63$	$p_1 = 65$	$p_1 = 60$
$s_4(t)$ (improved)	$c_1 = 0.75$	$c_1 = 0.8$	$c_1 = 0.82$
	$p_2 = 64$	$p_2 = 57$	$p_2 = 58$
	$c_2 = 0.7$	$c_2 = 0.75$	$c_2 = 0.78$

TABLE 8. Comparative BER performance of the fourth pulse, $s_4(t)$ ($p_1 = 60$, $c_1 = 0.85$), and the improved fourth pulse with those available in [25], for various values of $\tau \triangleq |t/T_b|$, SNR = 15dB.

α	Pulse		$\tau = 0.05$	Pulse		$\tau = 0.1$
0.25	0.64 0.62 0.56	$X_3(f)$	4.52×10^{-8}	0.68 0.64 0.56	$X_3(f)$	8.07×10^{-7}
		Spline 3	4.76×10^{-8}		Spline 3	8.95×10^{-7}
	(0.66,14)	$s_4(t)$	$\mathbf{4.58 \times 10^{-8}}$	(0.72, 20)	$s_4(t)$	$\mathbf{8.21 \times 10^{-7}}$
	(0.71, 56, 0.66, 62)	$s_4(t)$ (improved)	$\mathbf{4.55 \times 10^{-8}}$	(0.76, 65, 0.71, 64)	$s_4(t)$ (improved)	$\mathbf{8.10 \times 10^{-7}}$
	40 -100 85	Poly [22]	4.73×10^{-8}	40 -100 85	Poly [22]	8.83×10^{-7}
0.35	0.72 0.68 0.58	$X_3(f)$	3.03×10^{-8}	0.72 0.68 0.58	$X_3(f)$	3.48×10^{-7}
		Spline 3	3.20×10^{-8}		Spline 3	3.84×10^{-7}
	(0.72, 20)	$s_4(t)$	$\mathbf{3.07 \times 10^{-8}}$	(0.75, 25)	$s_4(t)$	$\mathbf{3.47 \times 10^{-7}}$
	(0.75, 63, 0.7, 64)	$s_4(t)$ (improved)	$\mathbf{3.04 \times 10^{-8}}$	(0.8, 65, 0.75, 57)	$s_4(t)$ (improved)	$\mathbf{3.43 \times 10^{-7}}$
	31 -80 69	Poly [22]	3.29×10^{-8}	31 -80 69	Poly [22]	3.84×10^{-7}
0.5	0.72 0.68 0.58	$X_3(f)$	1.92×10^{-8}	0.72 0.68 0.58	$X_3(f)$	1.23×10^{-7}
		Spline 3	2.01×10^{-8}		Spline 3	1.38×10^{-7}
	(0.75, 25)	$s_4(t)$	$\mathbf{1.92 \times 10^{-8}}$	(0.77, 30)	$s_4(t)$	$\mathbf{1.19 \times 10^{-7}}$
	(0.79, 60, 0.75, 64)	$s_4(t)$ (improved)	$\mathbf{1.91 \times 10^{-8}}$	(0.81, 64, 0.77, 63)	$s_4(t)$ (improved)	$\mathbf{1.18 \times 10^{-7}}$
	25 -64 55	Poly [22]	2.06×10^{-8}	25 -64 55	Poly [22]	1.35×10^{-7}

As far as the optimized PFE pulse is concerned, it achieves a slightly better performance than the improved fourth pulse for α of 0.25, α of 0.35 and all considered values of τ. For α of 0.5 and τ of 0.05 and 0.1, the performance gap between the improved fourth pulse and the optimized PFE is small. For larger values of τ the improved fourth pulse achieves an almost identical performance for τ of 0.2 and even slightly outperforms the optimized PFE pulse for τ of 0.3.

III. CONCLUSION

In this paper, we have proposed a new family of improved ISI-free pulses, the design of which is based on a geometric approach employing piece-wise cubic polynomials. The characteristics of the proposed pulses have been studied in terms of their frequency and time domain characteristics and their performance, in terms of BER and eye-diagram width has been analyzed. The proposed pulses have been

TABLE 9. Comparative BER performance of the fourth pulse, $s_4(t)$ ($p_1 = 60$, $c_1 = 0.85$) and the improved fourth pulse, with those available in [26, Table 6], for various values of $\tau \triangleq |t/T_b|$ and α with SNR = 15dB.

α	Pulse	$\tau = 0.05$	$\tau = 0.1$	$\tau = 0.2$	$\tau = 0.3$
0.25	poly	4.73×10^{-8}	8.83×10^{-7}	2.24×10^{-4}	1.01×10^{-2}
	power (b = 0.25)	4.58×10^{-8}	8.24×10^{-7}	2.05×10^{-4}	9.38×10^{-3}
	b (m = 0.24)	0.63	0.67	0.69	0.67
	CC3	4.55×10^{-8}	8.19×10^{-7}	2.00×10^{-4}	9.34×10^{-3}
	acos[asinh]	5.15×10^{-8}	9.98×10^{-7}	2.49×10^{-4}	1.14×10^{-2}
	b (m = 0.24)	0.67	0.72	0.74	0.72
	PFE	4.57×10^{-8}	8.23×10^{-7}	2.01×10^{-4}	9.38×10^{-3}
	{b, m} optimized	0.71653, 0.25	0.73226, 0.25	0.75905, 0.25	0.73673, 0.25
	PFE	4.51×10^{-8}	7.96×10^{-7}	1.91×10^{-4}	9.08×10^{-3}
	$s_4(t)$ (BER)	$\mathbf{4.58 \times 10^{-8}}$	$\mathbf{8.21 \times 10^{-7}}$	$\mathbf{1.98 \times 10^{-4}}$	$\mathbf{9.34 \times 10^{-3}}$
	$s_4(t)$ (c_2, p_2)	$(\mathbf{0.66}, \mathbf{14})$	$(\mathbf{0.72}, \mathbf{20})$	$(\mathbf{0.74}, \mathbf{23})$	$(\mathbf{0.72}, \mathbf{20})$
	$s_4(t)$ (improved, BER)	$\mathbf{4.55 \times 10^{-8}}$	$\mathbf{8.10 \times 10^{-7}}$	$\mathbf{1.96 \times 10^{-4}}$	$\mathbf{9.22 \times 10^{-3}}$
	$s_4(t)$, improved (c_1, p_1), (c_2, p_2)	$(\mathbf{0.71}, \mathbf{56})$, $(\mathbf{0.66}, \mathbf{62})$	$(\mathbf{0.76}, \mathbf{65})$, $(\mathbf{0.71}, \mathbf{64})$	$(\mathbf{0.78}, \mathbf{64})$, $(\mathbf{0.73}, \mathbf{60})$	$(\mathbf{0.76}, \mathbf{64})$,$(\mathbf{0.70}, \mathbf{63})$
0.35	poly	3.29×10^{-8}	3.84×10^{-7}	6.56×10^{-5}	4.07×10^{-3}
	power (b = 0.33)	3.10×10^{-8}	3.56×10^{-7}	6.43×10^{-5}	3.93×10^{-3}
	b (m = 0.34)	0.66	0.7	0.73	0.72
	CC3	3.05×10^{-8}	3.49×10^{-7}	5.99×10^{-5}	3.77×10^{-3}
	asech[asech]	3.22×10^{-8}	3.73×10^{-7}	6.41×10^{-5}	3.99×10^{-3}
	b (m = 0.34)	0.71	0.77	0.81	0.8
	PFE	3.05×10^{-8}	3.47×10^{-7}	5.88×10^{-5}	3.72×10^{-3}
	{b, m} optimized	0.73327, 0.35	0.77875, 0.35	0.81735, 0.35	0.81115, 0.35
	PFE	3.01×10^{-8}	3.38×10^{-7}	5.65×10^{-5}	3.60×10^{-3}
	$s_4(t)$ (BER)	$\mathbf{3.07 \times 10^{-8}}$	$\mathbf{3.47 \times 10^{-7}}$	$\mathbf{5.78 \times 10^{-5}}$	$\mathbf{3.67 \times 10^{-3}}$
	$s_4(t)$ (c_2, p_2)	$(\mathbf{0.72}, \mathbf{20})$	$(\mathbf{0.75}, \mathbf{25})$	$(\mathbf{0.79}, \mathbf{38})$	$(\mathbf{0.79}, \mathbf{38})$
	$s_4(t)$ (improved, BER)	$\mathbf{3.04 \times 10^{-8}}$	$\mathbf{3.43 \times 10^{-7}}$	$\mathbf{5.74 \times 10^{-5}}$	$\mathbf{3.65 \times 10^{-3}}$
	$s_4(t)$, improved (c_1, p_1), (c_2, p_2)	$(\mathbf{0.75}, \mathbf{63})$, $(\mathbf{0.7}, \mathbf{64})$	$(\mathbf{0.8}, \mathbf{65})$, $(\mathbf{0.75}, \mathbf{57})$	$(\mathbf{0.82}, \mathbf{60})$, $(\mathbf{0.78}, \mathbf{58})$	$(\mathbf{0.82}, \mathbf{60})$,$(\mathbf{0.78}, \mathbf{58})$
0.5	poly	2.06×10^{-8}	1.35×10^{-7}	1.52×10^{-5}	1.29×10^{-3}
	power (b = 0.37)	1.95×10^{-8}	1.25×10^{-7}	1.66×10^{-5}	1.62×10^{-3}
	b (m = 0.49)	0.7	0.73	0.77	0.78
	CC3	1.92×10^{-8}	1.22×10^{-7}	1.44×10^{-5}	1.24×10^{-3}
	asech[asech]	1.98×10^{-8}	1.29×10^{-7}	1.61×10^{-5}	1.48×10^{-3}
	b (m = 0.49)	0.77	0.8	0.86	0.88
	PFE	1.91×10^{-8}	1.19×10^{-7}	1.35×10^{-5}	1.17×10^{-3}
	{b, m} optimized	0.77882, 0.5	0.80648, 0.5	0.86457, 0.5	0.89202, 0.5
	PFE	1.89×10^{-8}	1.16×10^{-7}	1.31×10^{-5}	1.14×10^{-3}
	$s_4(t)$ (BER)	$\mathbf{1.92 \times 10^{-8}}$	$\mathbf{1.19 \times 10^{-7}}$	$\mathbf{1.30 \times 10^{-5}}$	$\mathbf{1.13 \times 10^{-3}}$
	$s_4(t)$ (c_2, p_2)	$(\mathbf{0.75}, \mathbf{25})$	$(\mathbf{0.77}, \mathbf{30})$	$(\mathbf{0.82}, \mathbf{64})$	$(\mathbf{0.82}, \mathbf{62})$
	$s_4(t)$ (improved, BER)	$\mathbf{1.91 \times 10^{-8}}$	$\mathbf{1.18 \times 10^{-7}}$	$\mathbf{1.30 \times 10^{-5}}$	$\mathbf{1.12 \times 10^{-3}}$
	$s_4(t)$, improved (c_1, p_1), (c_2, p_2)	$(\mathbf{0.79}, \mathbf{60})$, $(\mathbf{0.75}, \mathbf{64})$	$(\mathbf{0.81}, \mathbf{64})$, $(\mathbf{0.77}, \mathbf{64})$	$(\mathbf{0.82}, \mathbf{60})$, $(\mathbf{0.85}, \mathbf{64})$	$(\mathbf{0.87}, \mathbf{63})$,$(\mathbf{0.84}, \mathbf{61})$

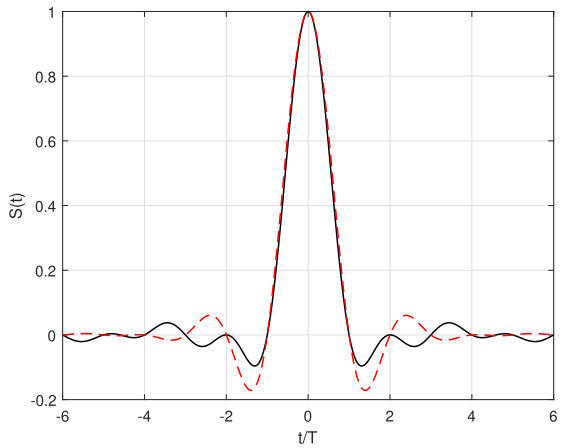

FIGURE 26. Impulse response of the fourth proposed pulse (continuous black line) and the RC pulse (dashed red line) for roll-off factor of 0.35, p_1 of 60, c_1 of 0.85, c_2 of 0.79 and p_2 of 38.

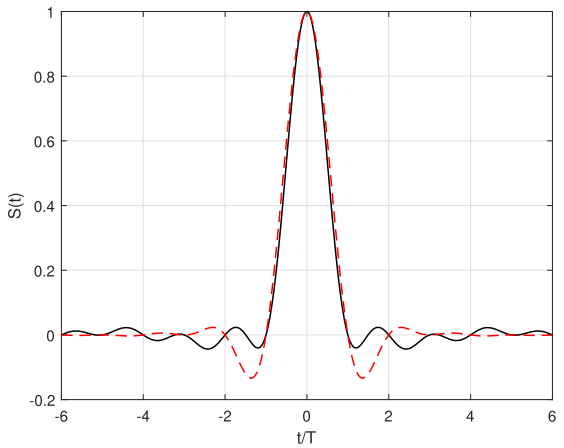

FIGURE 27. Impulse response of the fourth proposed pulse (continuous black line) and the RC pulse (dashed red line) for roll-off factor of 0.5, p_1 of 60, c_1 of 0.85, c_2 of 0.82 and p_2 of 64.

compared with the best so far two-parametric pulses reported in the open technical literature, namely the acsch[asech] [18], the acos[log] [16], [16] and the acos[asinh] [16], [16] as well as with more complicated pulse designs such as the polynomial [22], the power [23]. the parabolic (CC3) [19], the staircase and spline pulses [25] and the piecewise flipped

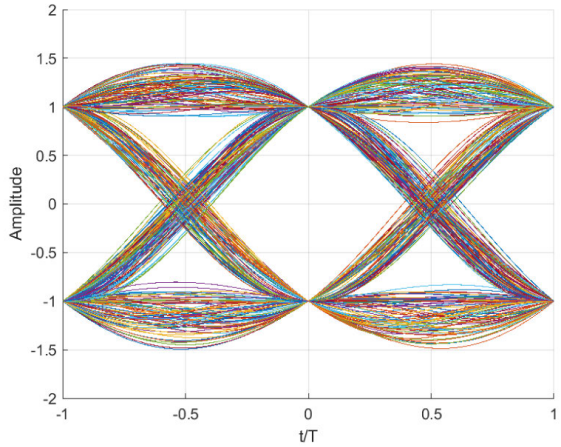

FIGURE 28. Eye diagram of the fourth proposed pulse for roll-off factor of 0.35, p_1 of 60, c_1 of 0.85, c_2 of 0.79 and p_2 of 38.

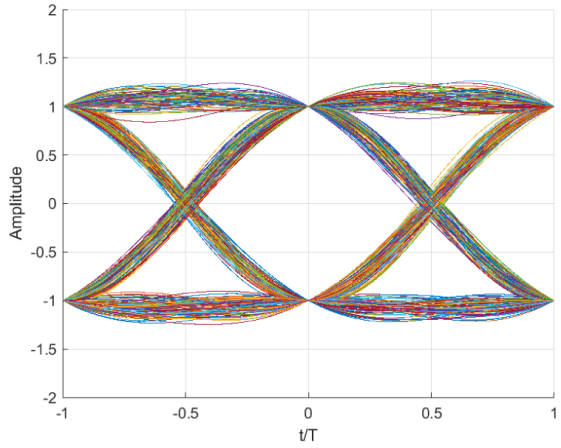

FIGURE 29. Eye diagram of the fourth proposed pulse for roll-off factor of 0.5, p_1 of 60, c_1 of 0.85, c_2 of 0.82 and p_2 of 64.

exponential (PFE) [26]. Note that two-parametric pulses achieve a reasonable tradeoff between error performance and implementation complexity whereas multi-parameter pulses achieve a better error performance at the cost of their implementation complexity, because optimization of their parameters may be required to yield the best performance. Our results have shown that the proposed pulses achieve an improved error rate performance in many cases and that the fourth member of the proposed family of pulses yields the best performance results. Specifically, the performance of this pulse is always better than the best so-far two-parametric pulses and comparable, or even better that the performance of best multi-parametric pulses, such as those proposed in [26]. Moreover, although the proposed family of pulses belongs to the category of multi-parameter pulses, their complexity is relatively low, thus rendering them suitable for efficient implementation and deployment in a hardware-based platform. The hardware implementation of the proposed pulses as well as their deployment on practical next generation communication systems are interesting and challenging topics which are left to a future research contribution.

REFERENCES

[1] M. Simsek, A. Aijaz, M. Dohler, J. Sachs, and G. Fettweis, "5G-enabled tactile Internet," *IEEE J. Sel. Areas Commun.*, vol. 34, no. 3, pp. 460–473, Mar. 2016.
[2] Z. Zhang, Y. Xiao, Z. Ma, M. Xiao, Z. Ding, X. Lei, G. K. Karagiannidis, and P. Fan, "6G wireless networks: Vision, requirements, architecture, and key technologies," *IEEE Veh. Technol. Mag.*, vol. 14, no. 3, pp. 28–41, Sep. 2019.
[3] H. Nyquist, "Certain topics in telegraph transmission theory," *Trans. Amer. Inst. Electr. Engineers*, vol. 47, no. 2, pp. 617–644, Apr. 1928.
[4] J. Proakis, *Digital Communications*, 4th ed. New York, NY, USA: McGraw-Hill, 2000.
[5] V. Kishore, V. M. Vakamulla, W. O. Popoola, and A. Kumar, "Implementation of linearly pulse shaped generalised frequency division multiplexing for visible light communication systems," *IEEE Open J. Commun. Soc.*, vol. 1, pp. 1614–1622, 2020.
[6] S. De, A. Misra, R. Das, T. Kleine-Ostmann, and T. Schneider, "Analysis of non-idealities in the generation of reconfigurable sinc-shaped optical Nyquist pulses," *IEEE Access*, vol. 9, pp. 76286–76295, 2021.
[7] S. De, K. Singh, C. Kress, R. Das, T. Schwabe, S. Preußler, T. Kleine-Ostmann, J. C. Scheytt, and T. Schneider, "Roll-off factor analysis of optical Nyquist pulses generated by an on-chip Mach–Zehnder modulator," *IEEE Photon. Technol. Lett.*, vol. 33, no. 21, pp. 1189–1192, Nov. 2021.
[8] H. Chen, J. Wang, H. Lu, T. Ning, L. Pei, and J. Li, "Reconfigurable optical frequency comb and Nyquist pulses generation with tunable sensitivities," *IEEE Access*, vol. 8, pp. 157211–157217, 2020.
[9] S. Liu, K. Wu, L. Zhou, G. Zhou, L. Lu, and J. Chen, "Modeling a dual-parallel silicon modulator for sinc-shaped Nyquist pulse generation," *IEEE J. Sel. Topics Quantum Electron.*, vol. 27, no. 3, pp. 1–8, May 2021.
[10] M. Shehata, K. Wang, J. Webber, M. Fujita, T. Nagatsuma, and W. Withayachumnankul, "Timing-jitter tolerant Nyquist pulse for terahertz communications," *J. Lightw. Technol.*, vol. 40, no. 2, pp. 557–564, Jan. 2022.
[11] M. Shehata, K. Wang, J. Webber, M. Fujita, T. Nagatsuma, and W. Withayachumnankul, "Mitigating the timing-jitter in terahertz communications via Nyquist pulse shaping," in *Proc. Opt. Fiber Commun. Conf. Exhib. (OFC)*, Mar. 2023, pp. 1–3.
[12] N. C. Beaulieu, C. C. Tan, and M. O. Dammen, "A 'better than' Nyquist pulse," *IEEE Commun. Lett.*, vol. 5, no. 9, pp. 367–368, Sep. 2001.
[13] N. C. Beaulieu and M. O. Damen, "Parametric construction of Nyquist-I pulses," *IEEE Trans. Commun.*, vol. 52, no. 12, pp. 2134–2142, Dec. 2004.
[14] X.-G. Xia, "A family of pulse-shaping filters with ISI-free matched and unmatched filter properties," *IEEE Trans. Commun.*, vol. 45, no. 10, pp. 1157–1158, Oct. 1997.
[15] A. Assalini and A. M. Tonello, "Improved Nyquist pulses," *IEEE Commun. Lett.*, vol. 8, no. 2, pp. 87–89, Feb. 2004.
[16] S. Assimonis, M. Matthaiou, and G. Karagiannidis, "Two-parameter Nyquist pulses with better performance," *IEEE Commun. Lett.*, vol. 12, no. 11, pp. 807–809, Nov. 2008.
[17] S. D. Assimonis, M. Matthaiou, G. K. Karagiannidis, and J. A. Nossek, "Improved parametric families of intersymbol interference-free Nyquist pulses using inner and outer functions," *IET Signal Process.*, vol. 5, no. 2, pp. 157–163, 2011.
[18] D. Tyrovolas, S. Liang, G. K. Karagiannidis, and S. D. Assimonis, "A novel two-parametric ISI-free pulse based on inverse hyperbolic functions," *IEEE Wireless Commun. Lett.*, vol. 12, no. 3, pp. 501–504, Mar. 2023.
[19] N. D. Alexandru and A. L. O. Balan, "Improved Nyquist filters with piece-wise parabolic frequency characteristics," *IEEE Commun. Lett.*, vol. 15, no. 5, pp. 473–475, May 2011.
[20] N. D. Alexandru and A. L. Balan, "ISI-free pulses produced by improved Nyquist filter with piece-wise linear characteristic," *Electron. Lett.*, vol. 47, no. 4, pp. 256–257, 2011.
[21] P. Sandeep, S. Chandan, and A. K. Chaturvedi, "ISI-free pulses with reduced sensitivity to timing errors," *IEEE Commun. Lett.*, vol. 9, no. 4, pp. 292–294, Apr. 2005.
[22] S. Chandan, P. Sandeep, and A. K. Chaturvedi, "A family of ISI-free polynomial pulses," *IEEE Commun. Lett.*, vol. 9, no. 6, pp. 496–498, Jun. 2005.
[23] M. Mohri and M. Hamamura, "ISI-free power roll-off pulse," *IEICE Trans. Fundam. Electron., Commun. Comput. Sci.*, vol. E92-A, no. 10, pp. 2495–2497, 2009.

[24] A. L. Balan and N. D. Alexandru, "Two improved Nyquist filters with piece-wise rectangular-polynomial frequency characteristics," *AEU-Int. J. Electron. Commun.*, vol. 66, no. 11, pp. 880–883, Nov. 2012.
[25] A. L. Onofrei and N. D. Alexandru, "Improved Nyquist filter characteristics using spline interpolation," *Ann. Telecommun.-Annales des télécommunications*, vol. 64, nos. 11–12, pp. 793–799, Dec. 2009.
[26] N. D. Alexandru and A. L. Balan, "ISI-free pulse with piecewise exponential frequency characteristic," *AEU-Int. J. Electron. Commun.*, vol. 70, no. 8, pp. 1020–1027, Aug. 2016.
[27] N. D. Alexandru and F. Diaconu, "Quick performance assessment of improved Nyquist pulses," *Wireless Commun. Mobile Comput.*, vol. 2017, Jan. 2017, Art. no. 7071648.
[28] U. A. K. Chude-Okonkwo, B. T. Maharaj, and R. Malekian, "Improving error probability performance of digital communication systems with compact Nyquist pulses," in *Proc. IEEE 2nd Wireless Afr. Conf. (WAC)*, Aug. 2019, pp. 1–6.
[29] X. Huang, H. Zhang, J. A. Zhang, Y. J. Guo, R.-L. Song, X.-F. Xu, C.-T. Wang, Z. Lu, and W. Wu, "Dual pulse shaping transmission with complementary Nyquist pulses," in *Proc. IEEE 90th Veh. Technol. Conf. (VTC-Fall)*, Sep. 2019, pp. 1–6.
[30] N. D. Alexandru and A. L. Balan, "Using apodization to boost the performance of improved Nyquist filters," in *Proc. 42nd Int. Conf. Telecommun. Signal Process. (TSP)*, Jul. 2019, pp. 41–44.
[31] Z. Zhou, L. Lin, and B. Jiao, "Auxiliary factor method to remove ISI of Nyquist filters," *IEEE Commun. Lett.*, vol. 27, no. 2, pp. 676–680, Feb. 2023.
[32] S. Traverso, "A family of square-root Nyquist filter with low group delay and high stopband attenuation," *IEEE Commun. Lett.*, vol. 20, no. 6, pp. 1136–1139, Jun. 2016.
[33] A. Kumar, M. Magarini, and S. Bregni, "Improving gfdm symbol error rate performance using 'better than Nyquist' pulse shaping filters," *IEEE Latin Amer. Trans.*, vol. 15, no. 7, pp. 1244–1249, Jun. 2017.
[34] A. Kumar, M. Magarini, and S. Bregni, "Impact of 'better than Nyquist' pulse shaping in GFDM PHY with LTE-compatible frame structure," in *Proc. IEEE 9th Latin-Amer. Conf. Commun. (LATINCOM)*, Nov. 2017, pp. 1–6.
[35] P. A. Haigh and I. Darwazeh, "Real time implementation of CAP modulation with 'better-than-Nyquist' pulse shaping in visible light communications," *IEEE Commun. Lett.*, vol. 24, no. 4, pp. 840–843, Jan. 2020.
[36] N. Sharma, A. Kumar, M. Magarini, S. Bregni, and D. N. K. Jayakody, "Impact of CFO on low latency-enabled UAV using 'better than Nyquist' pulse shaping in GFDM," in *Proc. IEEE 89th Veh. Technol. Conf. (VTC-Spring)*, Apr. 2019, pp. 1–6.
[37] N. D. Alexandru and A. L. Balan, "An analysis of improved Nyquist pulses based on Pearson distance," in *Proc. Int. Conf. Develop. Appl. Syst. (DAS)*, May 2018, pp. 83–87.
[38] J. H. Ahlberg, E. N. Nilson, and J. L. Walsh, *The Theory of Splines and Their Application*. New York, NY, USA: Academic, 1967.
[39] N. C. Beaulieu, "The evaluation of error probabilities for intersymbol and cochannel interference," *IEEE Trans. Commun.*, vol. 39, no. 12, pp. 1740–1749, Dec. 1991.

KYRIAKOS D. GAZOULEAS was born in Athens, Greece, in 1982. He received the bachelor's degree in mathematics from the National and Kapodistrian University of Athens, Greece, and the M.Sc. degree in advanced telecommunication systems and networks from the Department of Informatics and Telecommunications, University of Peloponnese, Tripolis, Greece. He was with the Department of Tissue Regeneration, MIRA–Institute for Biomedical Technology, University of Twente, Enschede, The Netherlands, in 3D culture modeling of metastatic breast cancer cells in additive manufactured scaffolds, and for the last years he has been working on digital communication systems.

NIKOS C. SAGIAS (Senior Member, IEEE) was born in Athens, Greece, in 1974. He received the B.Sc. degree from the Department of Physics, National and Kapodistrian University of Athens (UoA), Greece, in 1998, and the M.Sc. and Ph.D. degrees in telecommunication engineering from UoA, in 2000 and 2005, respectively.

From 2001 to 2010, he was involved in various national and European research and development projects with the Institute of Space Applications and Remote Sensing, National Observatory of Athens, Greece. From 2006 to 2008, he was a Postdoctoral Research Scholar with the Institute of Informatics and Telecommunications, National Centre for Scientific Research "Demokritos," Athens, Greece. From 2014 to 2016 and from 2018 to 2020, he was the Chair of the Department of Informatics and Telecommunications, University of Peloponnese, Tripoli, Greece, where he is currently a Professor. In the record, he has more than 60 articles in prestigious international journals and more than 50 papers in the proceedings of world-recognized conferences. His research interests include digital communications, and more specifically MIMO and cooperative systems, fading channels, mobile and satellite communications, optical wireless systems, and communication theory issues. He is a member of the IEEE Communications Society. He was a co-recipient of the Best Paper Award in PHY from the IEEE Wireless Communications and Networking Conference 2014 (WCNC14) and the 3rd International Symposium on Communications, Control and Signal Processing 2008 (ISCCSP08). Moreover, he has been serving as a TPC member for various IEEE flagship conferences, while from 2009 to 2014, he was an Associate Editor of the IEEE TRANSACTIONS ON WIRELESS COMMUNICATIONS

MICHAEL C. BATISTATOS received the bachelor's degree in physics from the Department of Physics, University of Ioannina, Greece, in 2000, and the M.Sc. degree in digital communications systems from the Department of Electronic and Electrical Engineering, Loughbourough University, U.K., in 2001. He was with the Institute of Informatics and Telecommunications, National Center for Scientific Research "Demokritos," Greece, participating in various telecommunications projects. He has been an IT and Telecommunications Teacher with private and public educational organizations. He received hands-on experience joining the leading telecommunications company Intracom Telecom as a Telecommunications Field Engineer. For the last ten years, he has been a Laboratory Teaching Staff Member with the Department of Informatics and Telecommunications, University of Peloponnese, Greece, with UAV communications as the main research interest.

KOSTAS P. PEPPAS (Senior Member, IEEE) was born in Athens, Greece, in 1975. He received the Diploma degree in electrical and computer engineering and the Ph.D. degree in wireless communications from the National Technical University of Athens, Athens, in 1997 and 2004, respectively. From 2004 to 2007, he was with the Department of Computer Science, University of Peloponnese, Tripolis, Greece, as a Researcher. From 2008 to 2014, he was also with the National Center for Scientific Research "Demokritos," Institute of Informatics and Telecommunications, as a Researcher. In 2014, he joined the Department of Telecommunication Science and Technology, University of Peloponnese, where he is currently a Lecturer. He has authored more than 100 journals and conference papers. His current research interests include digital communications over fading channels, MIMO systems, wireless and personal communication networks, and system-level analysis and design.